PRENATAL EXPOSURE TO ENVIRONMENTAL CHEMICALS MODULATES SERUM PHOSPHOLIPIDS IN NEWBORN INFANTS, INCREASING LATER RISK OF TYPE 1 DIABETES

***Running title*: Chemical exposure modifies neonatal metabolome and type 1 diabetes risk**

Aidan McGlinchey[1], Tim Sinioja[2], Santosh Lamichhane[3], Johanna Bodin[4], Heli Siljander[5], Dawei Geng[2], Cecilia Carlsson[2], Daniel Duberg[2], Jorma Ilonen[6,7], Suvi M. Virtanen[8,9], Hubert Dirven[4], Hanne Friis Berntsen[10,11], Karin Zimmer[10], Unni C. Nygaard[4], Matej Orešič[1,3,*], Mikael Knip[5,*], Tuulia Hyötyläinen[2,*]

[1]School of Medical Sciences, Örebro University, 702 81 Örebro, Sweden

[2]School of Science and Technology, Örebro University, 702 81 Örebro, Sweden

[3]Turku Centre for Biotechnology, University of Turku and Åbo Akademi University, 20520 Turku, Finland

[4]Division of Infection Control and Environmental Health, Norwegian Institute of Public Health, 0456 Oslo, Norway

[5]Children's Hospital, University of Helsinki and Helsinki University Hospital, 00290 Helsinki, Finland; Research Program for Clinical and Molecular Metabolism, Faculty of Medicine, University of Helsinki, 00290 Helsinki, Finland

[6]Immunogenetics Laboratory, Institute of Biomedicine, University of Turku, 20014 Turku, Finland

[7]Department of Clinical Microbiology, Turku University Hospital, 20014 Turku, Finland

[8]Public Health Promotion Unit, National Institute for Health and Welfare, 00271 Helsinki, Finland

[9]Center for Child Health Research, Tampere University Hospital, 33520 Tampere, Finland

[10]Norwegian University of Life Sciences, 0102 Oslo, Norway

[11]National Institute of Occupational Health, 0363, Oslo, Norway

*Shared senior authorship.

Correspondence:

Matej Orešič; Email: matej.oresic@utu.fi

Mikael Knip; Email: mikael.knip@helsinki.fi

Tuulia Hyötyläinen; MTM Research Centre, School of Science and Technology, Örebro University, 702 81 Örebro, Sweden. Email: tuulia.hyotylainen@oru.se; Phone: +46 19 303487

Abstract

In the last decade, the increasing incidence of type 1 diabetes (T1D) stabilized in Finland, coinciding with tighter regulation of per- and polyfluoroalkyl substances (PFAS). Here we applied lipidomics and quantification of PFAS to examine their effect, during pregnancy, on lipid-related markers of T1D risk in children. In a well-characterized mother-infant cohort (264 pairs), high PFAS exposure during pregnancy associated with decreased phospholipids in the offspring. This association was exacerbated with increased human leukocyte antigen-conferred risk of T1D in infants. Their lipid profiles proved similar to those observed in earlier studies in young children progressing to T1D later in life. Exposure to a single PFAS compound or a PFAS-containing mixture of organic pollutants in non-obese diabetic mice resulted in their offspring seeing a similar decrease in phospholipids, with early signs of insulitis. Our findings suggest that high PFAS exposure during pregnancy contributes to risk and pathogenesis of T1D in children.

INTRODUCTION

T1D is an autoimmune disease caused by destruction of insulin-secreting pancreatic beta-cells[1]. The strongest genetic risk factors for T1D are found within the human leukocyte antigen (HLA) gene complex[2], yet only 3-10% of individuals carrying HLA-conferred disease susceptibility develop T1D[3]. The role of environmental factors in T1D pathogenesis is thus obvious[4]. We previously found that children progressing to T1D later in life have a distinct lipidomic profile characterized by decreased blood phospholipid levels, including sphingomyelins (SMs), within the first months of life, preceding the onset of islet autoimmunity[5, 6] and even as early as at birth[7, 8]. The cause of these metabolic changes is currently poorly understood. The gut microbiome is known to affect host lipid metabolism[9] and is associated with progression to T1D[10, 11], particularly in the period after islet seroconversion, but current data does not offer an explanation for the earlier changes in phospholipid levels[10].

The incidence of T1D has been increasing over the last decades in many industrialized countries[12]. However, for unknown reasons, this has stabilized in the last decade, particularly in the Nordic countries[13, 14]. Environmental triggers are often implicated in T1D, such as enterovirus infection, diet, and obesity[4], yet these do not explain this observation. Obesity, for example, has not shown a concomitant decrease since 2005[15], and the number of severe enterovirus infections in Finland 2006-2010 increased, in fact, 10-fold[14].

Notably, the time trend of human exposure levels to two widely-used industrial chemicals, namely, perfluorooctane sulfonate and perfluorooctanoic acid (PFOS and PFOA), do coincide with this trend of T1D incidence[14]. These two compounds belong to a group of PFAS which are widely-used in food packaging materials, paper and textile coatings, and fire-fighting foams[16]. The use of PFOS and PFOA has increased substantially from when production started in the 1950s until the main, global manufacturer phased out its production of PFOS, PFOS-related substances and PFOA between 2000-2002. In the European Union, all uses of PFOS are now prohibited under Directive (2006/122/EC) which came into force in 2008. PFOA is still manufactured and a large number of other PFAS compounds are currently in use. With a half-life up to a decade long in humans, concentrations of PFOS and PFOA in humans started to decrease only after *ca*. 2005, with the levels of many other PFAS still showing increasing trends[17, 18]. The main sources of exposure to PFAS in the general population are food and drinking water, with lesser sources including house dust and air. PFAS are transferred from mother to fetus *via* the placenta and to breast-fed infants *via* maternal milk[19].

There is a dearth of knowledge regarding PFAS as possible triggers for T1D, although contribution to the development of T1D has been proposed *via* impaired beta/immune-cell functions and immunomodulation[20]. It has been shown that PFOA and PFOS disrupt generation of human pancreatic progenitor cells[21]. Prenatal and early-life exposure to perfluoroundecanoic acid (PFUnDA) aggravates

insulitis development in NOD mice[22]. Recently, elevated levels of PFOS were reported in children at the onset of T1D[23].

Here we hypothesized that PFAS exposure *in utero* affects the phospholipid profile of newborn infants and explains the association between phospholipids and increased T1D risk. In a mother-infant cohort study, we analyzed metabolite profiles of pregnant mothers and their offspring at birth and quantified selected PFAS in maternal samples during pregnancy. We then further experimentally examined the impact of PFAS exposure on metabolite profiles and the development of insulitis / autoimmune diabetes in NOD mice.

RESULTS

Metabolomic analyses of the mother-infant cohort

A total of 264 mother-infant dyads were included in the study (**Figure 1**; **Supplementary Table 1**). Delivery age was between 18.5 and 45.8 years, pre-pregnancy BMI was between 23.4 and 45.7 kg/m², with 62% of the mothers being normal weight (BMI 18.5-25). All babies were born after gestational week 35.

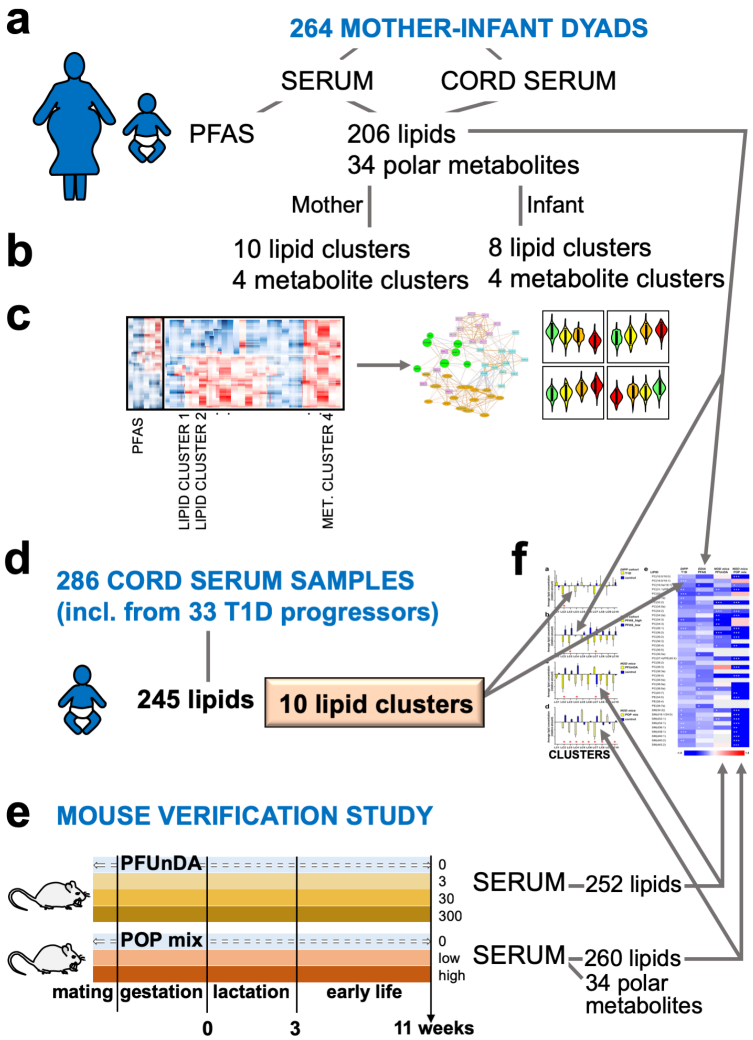

Figure 1. Overview of the workflow integrating prenatal PFAS exposure assessment, serum metabolomics and risk of type 1 diabetes. **a**. In a mother-infant cohort, PFAS levels and metabolomic profiles were determined from pregnant mothers, and metabolomics performed on cord serum from newborn infants. **b**. Metabolites were summarized as clusters, and (**c**) associations between prenatal PFAS exposure and metabolomes were studied. Cord serum lipid changes due to prenatal PFAS exposure were then compared to (**d**) previously reported[7] lipid-related differences between newborn infants who progressed to T1D later in life *vs.* those that remained healthy (Type 1 Diabetes Prediction and Prevention study – DIPP), and to (**e**) changes in lipid profiles brought on by exposure to a single PFAS compound or mixture of persistent organic pollutants, respectively, from two studies in non-obese diabetic (NOD) mice. **f**. The data across the four different studies (**a**, **d**, **e**) were summarized and compared by assigning lipids from each respective study to lipid clusters from the T1D study[7].

Serum concentrations of 25 PFAS compounds were determined in the mothers during the pregnancy, using pooled samples collected at two time points, one during pregnancy and one at delivery (**Supplementary Table 2**). The two most abundant PFAS were PFOS and PFOA, detected in all subjects. Our detected levels of PFOS and PFOA were lower than reported in previous studies[18], most of which used samples collected before 2010, and therefore before recent, noted decreases in population levels of PFOS and PFOA[24].

Metabolomic analyses were performed using two analytical platforms. Serum molecular lipids and polar metabolites were quantified from the mothers during pregnancy and from newborn infants (cord serum). A total of 206 lipids and 34 polar metabolites were included in the final datasets. To reduce dimensional complexity and facilitate identification of global associations between metabolic profiles and maternal PFAS exposure, we first clustered the metabolites from all datasets into cluster variables using model-based clustering[25], followed by partial-correlation network analysis[26]. This resulted in ten Mother Lipid Clusters (MLCs) and four Mother polar Metabolite Clusters (MMCs) (**Supplementary Table 3**), while the cord serum lipidomics data yielded eight Child Lipid Clusters (CLCs) and four Child polar Metabolite Clusters (CMCs) (**Supplementary Table 4**).

Metabolic profiles in mothers associate with PFAS exposure

PFAS exposure impacted the maternal metabolome (**Figure 2**), both at the cluster variable level as well as at the individual metabolite level. Total PFAS as well as several individual PFAS levels were positively associated with MMC1 (amino acids, saturated free fatty acids and cholesterol). At the individual metabolite level, a positive correlation with total PFAS was also observed for octanoic and decanoic acids as well as lysine and alanine. Although no strong association was observed between the maternal lipid clusters and PFAS exposure, the levels of total PFAS were positively associated with individual lipids such as phosphatidylcholines (PCs) containing polyunsaturated fatty acyls (PUFA), and a trend of positive association with saturated fatty acyl-containing triacylglycerols (TGs), ceramides as well as diacylglycerols (DGs) was observed.

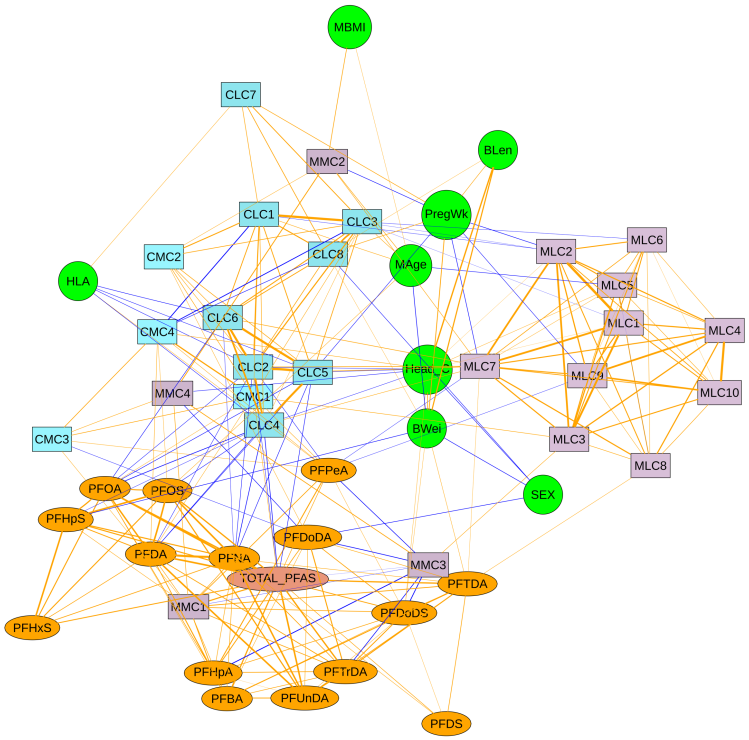

Figure 2. Partial correlation network showing associations between demographic data, maternal PFAS levels and lipidome / metabolome cluster variables from mothers and their newborn infants. The network was constructed using the qpgraph R package[26]. Node color represents different types of variables, edge color denotes a positive (orange) or negative (blue) association. The threshold non-rejection rate was set as 0.5. Node abbreviations: PregWk, weeks of pregnancy; HLA, HLA risk locus (1 = lower risk, 2 = higher risk); Head_C, head circumference of child; BWei, birth weight; BLen, birth length; MBMI, mother's BMI; MAge, mother's age.

For a subset of the cohort (n = 116), detailed lifestyle data, including dietary data during pregnancy, were available, and this dataset was used to estimate dietary sources of PFAS (**Supplementary Figure 2**). Shellfish showed the strongest correlation with serum PFAS levels, with other food items also showing significant associations with the PFAS levels, such as fish, cereals and fruit juice. Fish oil consumption, which is not associated with PFAS exposure[27], increases serum levels of phospholipids and TGs containing PUFA[28].

Conversely, PFAS exposure is associated with increased levels of these lipids[29]. This suggests that, to a large extent, seafood consumption drives maternal PFAS levels.

Cord serum profiles in newborn infants associate with PFAS exposure

Partial correlation network analysis revealed a marked impact of maternal PFAS exposure on the cord serum metabolome of newborn infants (**Figure 2**). Inverse associations between cord serum lipids and PFOS, PFOA and total PFAS exposure were observed, particularly for clusters CLC2 (PUFA-containing phosphatidylcholines/PCs), CLC4 (lysophosphatidylcholines/LPCs) and CLC5 (sphingomyelin, abundant PCs). CMC4 (mainly specific amino acids) was positively associated with PFOS and perfluorodecanoic acid (PFDA) exposure.

Next, the infants were classified into four groups (quartiles) based on total maternal PFAS exposure levels during the pregnancy, as a sum of all measured PFAS exposures. Among the eight CLCs and four CMCs, one lipid cluster (CLC4) and one polar metabolite cluster (CMC4) were significantly different between the highest (Q4) and lowest (Q1) PFAS exposure quartiles, with two additional clusters close to significance (CLC5 and CMC1) (**Supplementary Table 5**). At the individual metabolite level, several lipid species including LPCs, PCs, SMs and TGs were downregulated as total exposure increased. Specific amino acids, including phenylalanine, methionine and aspartic acid were significantly upregulated in the highest exposure group (**Figure 3**, **Supplementary Table 6**).

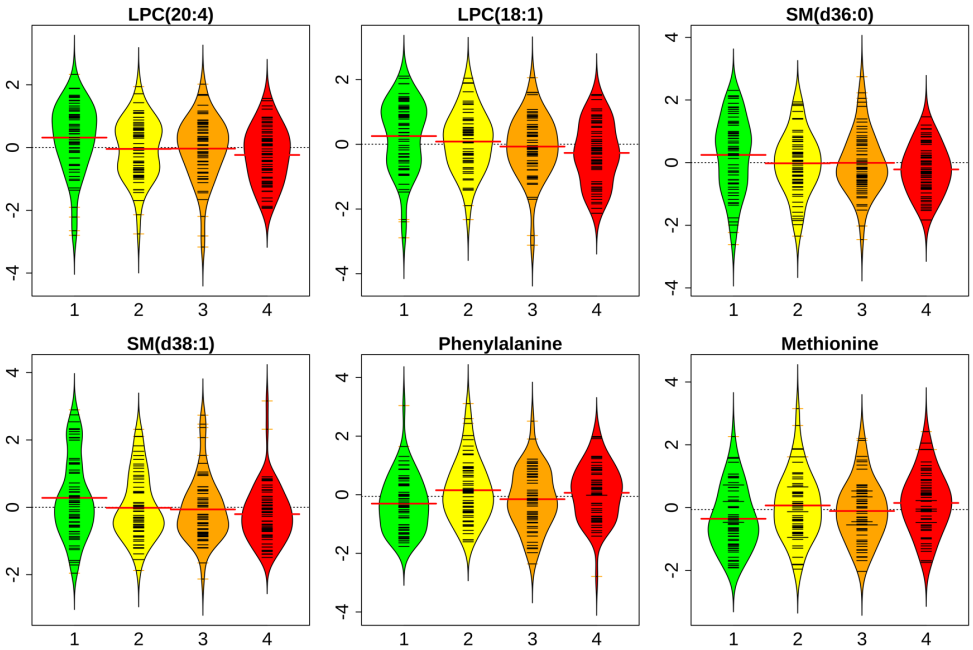

Figure 3. Beanpots showing levels of four selected lipids and two polar metabolites, measured in cord serum, having significant (adjusted $p < 0.05$) associations with total maternal prenatal PFAS exposure (**Supplementary Table 6**). X-axis numbers correspond to total maternal PFAS exposure level from lowest (1) to highest (4) quartile. Red, horizontal bars indicate means, black horizontal bars are individual sample values and "bean" width represents the density of samples occurring at that level. All values plotted are log2 transformed and scaled to zero mean and unit variance.

We then studied the associations between the matched maternal and cord serum metabolite levels using Spearman correlation. Following multiple hypothesis correction, only four lipids remained significantly correlated between the mothers and offspring. However, the correlation between the lipids was low overall ($|R| < 0.24$). Polar metabolites showed no significant correlations.

Impact of PFAS exposure on cord serum lipids associated with T1D progression

As the cord serum lipid profile associated with total maternal PFAS exposure here proved similar to that found previously as being associated with progression to T1D[7], we also examined the impact of PFAS

exposure on T1D-associated lipids. First, we assigned the lipids from the present study to the same lipid clusters (LCs) as used in our previous study, and investigated their association with PFAS levels.

Of the ten lipid clusters used in the earlier study, five showed significant differences between the highest and lowest exposure groups (**Supplementary Table 7**). In our previous study, the most significantly-changing lipid clusters associated with T1D progression were LC2 (major PCs) and LC7 (sphingomyelins), which were down-regulated in newborn infants who later progressed to clinical T1D. In agreement with these results, the lipid levels in those same clusters in the present study were also significantly lower in the highest (Q4) exposure group by comparison to the lowest (Q1) exposure levels. In addition, lipid clusters LC3 (LPCs) and LC6 (PUFA containing phospholipids) showed clear differences in the current study, with lower lipid levels seen in the highest exposure group.

Of the 15 top-ranked lipids reported to have significant associations with T1D development[7], seven of these showed significant association with total PFAS exposure ($p < 0.05$). All of the others lipids showed marginally-significant differences ($p < 0.08$) (**Supplementary Table 8**). Among the individual PFAS, the strongest association was observed for PFNA, with all 15 cord serum lipids being significantly associated with the prenatal PFNA exposure.

Given the observed impact of prenatal exposure to PFAS on cord serum lipids associated with progression to T1D, we also examined whether HLA-conferred risk of T1D plays a role in mediating the impact of PFAS exposure on lipids in newborn infants. We divided the babies into two categories according to HLA-associated T1D risk: (low *vs.* increased; **Supplementary Table 1**) and two categories according to prenatal total PFAS exposure (quartiles 1 & 2 *vs.* 3 & 4). Two-way ANOVA was then performed across these groups for the eleven lipids found associated with PFAS exposure. When examining the interaction effect between HLA risk and PFAS exposure, we found four lipids with p-value < 0.05, and five more lipids with $p < 0.12$ (**Supplementary Table 9**).

Pre- and postnatal PFAS exposure in NOD mice alters offspring lipid profiles

Based on the metabolomics results from the mother-infant cohort, we hypothesized that PFAS exposure during pregnancy has a causal impact on phospholipid levels, which, in turn, associate with increased risk of T1D. Two previously-reported studies in NOD mice suggest that maternal PFAS exposure accelerates insulitis development and progression to autoimmune diabetes[22, 30]. We analyzed serum lipidomic profiles from these two studies, being (1) NOD mice (11 weeks of age) with exposure either to PFUnDA in drinking water (3, 30 and 300 μg/l)[22] or (2) to a mixture of persistent organic pollutants (POPs) in feeds at low and high levels (total intake for PFAS of 0.14 μg/day (low) or 2.8 μg/day (high), with the low level corresponding to the approximate human PFAS serum levels and high representing a 50-times higher total PFAS serum levels[31, 32, 33]). These doses occurred at the times of mating, during gestation and lactation and until 11 weeks of age[30]. We also measured polar metabolites in the latter mouse study.

Exposure to PFUnDA caused significant changes in lipid profiles at the highest exposure concentration, with similar patterns of changes found with the two lower concentrations, although these did not reach statistical significance (**Supplementary Table 10**). Marked changes were, however, observed in the second study, where mice were exposed to the POP mixture, with the strongest effects seen in the high exposure group, but with significant changes still occurring also in the low exposure group which corresponds to expected human exposure levels (**Supplementary Table 11**). Specifically, exposure caused a marked reduction of a large number of phospholipids, with several PUFA-containing TGs being significantly down-regulated as well. We also identified significant changes in the levels of several free fatty acids, free cholesterol, amino acids, glycerol-3-phosphate and 3-hydroxybutyric acid, particularly in the high exposure group, with significant upregulation of TCA cycle metabolites.

Next, we assigned the measured lipids to the same lipid clusters (LCs) as in our previous study[7] and investigated the association of PFAS exposure with these lipid clusters. Of the ten lipid clusters, four showed significant differences between the highest PFUnDA-exposure group and the control mice. One lipid cluster showed a significant difference even at the lowest level of exposure compared to control. In

mice exposed to the POP mixture, eight of ten clusters showed significant changes between control and high exposure groups, and two clusters changed significantly between control and low exposure groups. In agreement with our previous study and our mother-infant cohort study presented here, LC2 decreased significantly with increasing PFAS exposure. In addition, clusters LC4, LC9 and LC10 showed clear differences in the current study with significantly lower lipid levels in the highest exposure group. These clusters contained mainly minor phospholipids, major TGs and long-chain TGs with PUFAs. Using the cluster assignments from the earlier study[7], a remarkable similarity was observed when comparing the results across all four studies (**Figure 4**): (1) a previously-reported study of the cord serum lipidome in relation to progression to T1D[7], (2) the association between PFAS exposure and cord serum lipid profiles in the mother-infant cohort presented here, and (3) the effects of PFUnDA and (4) a PFAS-containing POP mixture on the lipid profiles of NOD mice. Among the 15 individual lipids reported to have significant association with the development of T1D, 11 and 10 of these were detected also in the NOD mice, exposed to PFUnDA and POP mixture, respectively. Of these lipids, three showed significant differences between control and high exposure groups in the PFUnDA model and nine in the POP mixture exposure model. Notably, the pattern of the changes in the two mouse models were very similar, indicating that the PFAS mixture was driving the differences also in the POP mixture model. All lipid changes taking place in association with higher PFAS exposure occurred in the same direction as reported previously in relation to higher risk of T1D.

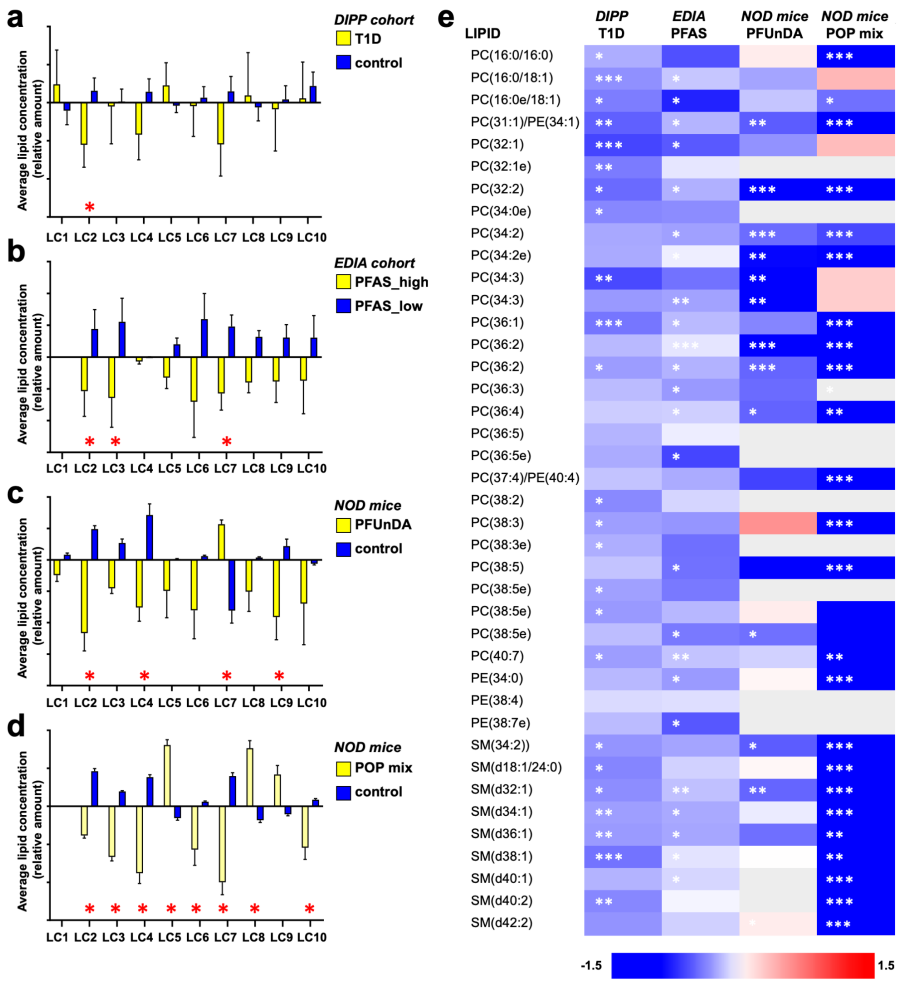

Figure 4. Comparison of lipidomic profiles across four different studies, using lipid cluster assignments from an earlier study[7]. **a**. Cord serum profiles from progressors to T1D (blue bars) and control children (yellow bars), from a previous report in the Diabetes Prediction and Prevention (DIPP) study in Finland[7]. **b**. Cord serum from mother-infant (EDIA) cohort, with high PFAS exposure (blue) and low exposure (yellow). **c**. NOD mice exposed to a high level of PFUnDA (blue) and unexposed control mice (yellow). **d**. NOD mice exposed to POP mixture at a high level (blue) and unexposed mice (yellow). **e**. Fold changes between the groups in **a-d** of lipids in cluster LC2. Statistical significance levels: *p<0.05, **p<0.01, ***p<0.001.

DISCUSSION

By integrating PFAS exposure and metabolomic data from pregnant mothers with metabolomic data from their newborn infants, we were able to demonstrate altered cord serum metabolic signatures associated with high PFAS exposure during pregnancy and subsequently verify these in NOD mouse models of pre- and postnatal PFAS exposure. We also reported a remarkable similarity between the metabolic signature observed in the current (EDIA) study and the known signature associated with progression to T1D.

The composition of the cord blood metabolome reflects maternal metabolism, placental transfer across the maternal-fetal axis as well as fetal metabolism itself[34]. This may explain the weak associations between metabolic profiles of mothers and their offspring. The observed PFAS-associated metabolic changes seen in cord blood were not associated with PFAS-related maternal metabolic changes. These fetal metabolic changes are therefore likely the result of PFAS exposure itself, rather than a downstream consequence of maternal metabolic changes. Several studies have shown that maternal levels of PFAS are reflected in the developing fetus[35] and there is a strong correlation between PFAS levels in maternal and cord blood[36]. One recent study indicates that PFAS concentrations in first trimester fetuses represent 5% to 27% of maternal plasma concentrations, fetal concentrations increasing with gestational age[37]. A comparison of transplacental transfer efficiency (TTE) for different PFAS suggests an inverse relationship with the chain-length of the perfluoroalkyl group and a somewhat lower transfer efficiency for perfluorosulfonic acids compared to perfluorocarboxylic acids[35]. We did not determine PFAS levels in newborn infants due to the limited volumes of samples available for quantification.

There is general consensus that exposure to PFOA and PFOS alters the immune system in experimental models, with documented effects including altered antibody and cytokine production[38]. In our study, we observed that prenatal PFAS exposure caused decreased levels of several phospholipids, particularly SMs and specific PCs, which were previously found to be persistently down-regulated in children who later progressed to clinical T1D[5, 6]. The importance of sphingolipid metabolism in the pathogenesis of T1D was recently highlighted by a genome-wide association study (GWAS) which identified eight gene polymorphisms involved in sphingolipid metabolism that contribute to T1D predisposition, and levels of which also correlated with the degree of islet autoimmunity in patients with recent-onset T1D[39]. Among the PFAS measured in our study, the main drivers of observed changes in cord serum phospholipid levels were PFNA, PFOS, PFUnDA and PFOA. Also, serine and palmitic acid (precursors of SMs) were found to be down-regulated in mothers with higher PFAS exposure and correlated with SM levels ($R > 0.4$), both in newborn infants as well as in NOD mice, where the exposure to PFAS was also associated with accelerated insulitis development[22]. We conclude that high PFAS exposure may alter sphingolipid levels during fetal development which may then go on to play a pathogenic role in the development of T1D later in life. The potential role of HLA-associated T1D risk in exacerbating the effect of prenatal PFAS exposure on lipid levels in the offspring, as suggested by our data, clearly demands further investigation.

Taken together, we conclude that high prenatal exposure to PFAS appears to alter lipid profiles in newborn infants, which, in turn, may increase the risk of T1D. Our data also highlight a potential role for a gene-environment interaction (HLA risk genotype and prenatal PFAS exposure), which may lead to altered lipid profiles in newborn infants at-risk of developing T1D. Our findings may offer an explanation for the changing trend in the incidence of T1D in Western countries as well as underscore the need for investigations of how exposures to specific PFAS and other persistent chemical pollutants during pregnancy and early childhood affect the risk and pathogenesis of T1D.

METHODS

Mother-infant cohort

Pregnant women were recruited from January 28, 2013 to February 26, 2015, in the context of the EDIA (Early Dietary Intervention and Later Signs of Beta-Cell Autoimmunity: Potential Mechanisms) study, which is a small-scale intervention trial comparing weaning infants onto an extensively-hydrolyzed milk formula *vs.* a conventional cow's milk-based formula. Families were contacted at the time of the fetal ultrasonography visit, which is arranged for all pregnant women in Finland around gestational week 20. Written, informed consent was signed by the parents to permit analysis of their HLA genotype to exclude infants without HLA-conferred susceptibility to T1D. At this point, 68% of the infants to be born were excluded. Separate informed consent was obtained from eligible parents at the beginning of the third trimester to analyze the offspring's genotype and to continue in the intervention study.

The cord blood from 309 newborn infants was screened to determine the HLA genotype, as previously described[40]. The degree of HLA susceptibility to T1D was divided into six categories (high-risk, moderate-risk, low-risk, neutral, protective and strongly protective genotypes), as earlier presented[41]. A total of 89 infants were eligible for participation in the intervention study, carrying high-risk and moderate-risk genotypes. In that study, 82 infants were randomized and 73 remained in follow-up up until the age of 12 months.

For the current study, the HLA risk categories were combined into two classes; the increased risk genotypes and the low-risk genotypes. Genotypes where HLA-(DR3)-DQA1*05-DQB*02 and/or DRB1*04:01/2/4/5-DQA1*03-DQB1*03:02 were present with each other, homozygous or heterozygous with a neutral haplotype were classified as increased risk and all other genotypes as low risk. Maternal diet during pregnancy was assessed by validated semiquantitative food frequency questionnaire[42]. Food and individual nutrient intakes were calculated using the national food composition database, Fineli[43]. We had access to 329 maternal serum samples collected at the beginning of the third trimester and 274 samples taken at delivery. We had altogether 300 cord blood samples. By pairing maternal and cord blood samples we obtained with 264 paired mother-infant samples.

NOD mouse study – summary

The study setting of the two NOD mouse studies mice was reported previously[22, 30]. In short, NOD/ShiLtJ mice from the Jackson Laboratory (Maine, USA) were used for breeding at 8 and 10 weeks of age and randomly allocated to the exposure groups. Female offspring were, in both studies, exposed at mating, through gestation and early life until 11-12 weeks of age when the serum samples were collected, with 4-5 mice kept per cage and 5-8 mice per exposure group.

The exposure in the first study was to PFUnDA in the drinking water (n=8 per group) (0, 3, 30 and 300 µg/l, corresponding to 0.417, 4.17 and 41.7 µg/kg bw/day). The lowest exposure level of PFUnDA is about five times higher than the maximal calculated intake of PFOA in human infants. The exposure in the second study (n=5 per exposure group) was to a mixture of persistent organic pollutants in feed, with a high and a low dose mixture (chemical composition based on human intake[30, 32]). The total intake of PFAS was 0.14 µg/day and 2.8 µg/day from the low and high dose groups respectively, corresponding to (1) human serum levels of PFAS and (2) 50 times the human serum levels. In both studies, the mice had *ad libitum* access to food and water (Harlan Teklad 2919 irradiated, Madison, WI) and had a 12 h light/12 h dark cycle with 35–75% humidity.

All experiments were performed in conformity with the laws and regulations for experiments with live animals in Norway and were approved by the local representative of the Norwegian Animal Research Authority. Insulitis was assessed by grading of hematoxylin and eosin-stained pancreatic tissue sections. Early signs of insulitis included an increased number of apoptotic cells, a decreased number of tissue-resident macrophages in pancreatic islets and reduced phagocytic function of macrophages isolated from the peritoneum.

Analyses of PFAS

Sample preparation and analysis for PFAS was carried out as described previously[44]. In short, 450 µL acetonitrile with 1% formic acid, and internal standards were added to 150 µL serum and samples subsequently treated with Ostro sample preparation in a 96-well plate for protein precipitation and phospholipid removal. The analysis of PFAS was performed using automated column-switching ultra-performance liquid chromatography-tandem mass spectrometry (UPLC-MS/MS) (Waters, Milford, USA) using an Acquity C18 BEH 2.1×100mm×1.7µm column and a gradient with 30% methanol in 2mM NH4Ac water and 2mM NH4Ac in methanol with a flow rate of 0.3 ml/min. Quantitative analysis of the selected analytes was performed using the isotope dilution method; all standards (*i.e.*, internal standards, recovery standards, and native calibration standards) were purchased from Wellington Laboratories (Guelph, Ontario, Canada). The method's detection limits ranged between 0.02-0.19 ng/mL, depending on the analyte.

Analysis of molecular lipids by UHPLC-QTOFMS

Serum samples were randomized and extracted using a modified version of the previously published Folch procedure[45]. In short, 10 µL of 0.9% NaCl and, 120 µL of CHCl3: MeOH (2:1, v/v) containing the internal standards (c = 2.5 µg/mL) was added to 10 µL of each serum sample. The standard solution contained the following compounds: 1,2-diheptadecanoyl-sn-glycero-3-phosphoethanolamine (PE(17:0/17:0)), N-heptadecanoyl-D-erythro-sphingosylphosphorylcholine (SM(d18:1/17:0)), N-heptadecanoyl-D-erythro-sphingosine (Cer(d18:1/17:0)), 1,2-diheptadecanoyl-sn-glycero-3-phosphocholine (PC(17:0/17:0)), 1-heptadecanoyl-2-hydroxy-sn-glycero-3-phosphocholine (LPC(17:0)) and 1-palmitoyl-d31-2-oleoyl-sn-glycero-3-phosphocholine (PC(16:0/d31/18:1)), were purchased from Avanti Polar Lipids, Inc. (Alabaster, AL, USA), and, triheptadecanoylglycerol (TG(17:0/17:0/17:0)) was purchased from Larodan AB (Solna, Sweden). The samples were vortex mixed and incubated on ice for 30 min after which they were centrifuged (9400 × g, 3 min). 60 µL from the lower layer of each sample was then transferred to a glass vial with an insert and 60 µL of CHCl3: MeOH (2:1, v/v) was added to each sample. The samples were re-randomized and stored at -80 °C until analysis.

Calibration curves using 1-hexadecyl-2-(9Z-octadecenoyl)-sn-glycero-3-phosphocholine (PC(16:0e/18:1(9Z))), 1-(1Z-octadecenyl)-2-(9Z-octadecenoyl)-sn-glycero-3-phosphocholine (PC(18:0p/18:1(9Z))), 1-stearoyl-2-hydroxy-sn-glycero-3-phosphocholine (LPC(18:0)), 1-oleoyl-2-hydroxy-sn-glycero-3-phosphocholine (LPC(18:1)), 1-palmitoyl-2-oleoyl-sn-glycero-3-phosphoethanolamine (PE(16:0/18:1)), 1-(1Z-octadecenyl)-2-docosahexaenoyl-sn-glycero-3-phosphocholine (PC(18:0p/22:6)) and 1-stearoyl-2-linoleoyl-sn-glycerol (DG(18:0/18:2)), 1-(9Z-octadecenoyl)-sn-glycero-3-phosphoethanolamine (LPE(18:1)), N-(9Z-octadecenoyl)-sphinganine (Cer(d18:0/18:1(9Z))), 1-hexadecyl-2-(9Z-octadecenoyl)-sn-glycero-3-phosphoethanolamine (PE(16:0/18:1)) from Avanti Polar Lipids, 1-Palmitoyl-2-Hydroxy-sn-Glycero-3-Phosphatidylcholine (LPC(16:0)) from Larodan, and 1,2,3 trihexadecanoalglycerol (TG(16:0/16:0/16:0)), 1,2,3-trioctadecanoylglycerol (TG(18:0/18:0/18:)) and 3β-hydroxy-5-cholestene-3-stearate (ChoE(18:0)), 3β-Hydroxy-5-cholestene-3-linoleate (ChoE(18:2)) from Larodan, were prepared to the following concentration levels: 100, 500, 1000, 1500, 2000 and 2500 ng/mL (in CHCl3:MeOH, 2:1, v/v) including 1250 ng/mL of each internal standard.

The samples were analyzed by ultra-high-performance liquid chromatography quadrupole time-of-flight mass spectrometry (UHPLC-QTOFMS)[46]. Briefly, the UHPLC system used in this work was a 1290 Infinity system from Agilent Technologies (Santa Clara, CA, USA). The system was equipped with a multi sampler (maintained at 10 °C), a quaternary solvent manager and a column thermostat (maintained at 50 °C). Separations were performed on an ACQUITY UPLC® BEH C18 column (2.1 mm × 100 mm, particle size 1.7 µm) by Waters (Milford, MA, USA). The mass spectrometer coupled to the UHPLC was a 6545 QTOF from Agilent Technologies interfaced with a dual jet stream electrospray (dual ESI) ion source. All analyses were performed in positive ion mode and MassHunter B.06.01 (Agilent Technologies) was used for all data acquisition. Quality control was performed throughout the dataset by including blanks, pure

standard samples, extracted standard samples and control serum samples. Relative standard deviations (% RSDs) for peak areas for lipid standards representing each lipid class in the control serum samples (n= 12) and in the pooled serum samples (n = 77) were calculated on average 15.9% and 13.6% (raw variation) in maternal samples and in cord blood samples, respectively. For serum samples from NOD mice, RSD was on average 11.9%. The lipid concentrations in pooled control samples showed % RSDs within accepted analytical limits at averages of 14.7% and 20.4% for the maternal and cord blood serum samples, respectively, and 7.3% for serum samples from NOD mice.

Mass spectrometry data processing was performed using the open source software package MZmine 2.18[47]. The following steps were applied in this processing: (1) Crop filtering with a m/z range of 350 – 1200 m/z and an RT range of 2.0 to 12 minutes, (2) Mass detection with a noise level of 750, (3) Chromatogram builder with a minimum time span of 0.08 min, minimum height of 1000 and a m/z tolerance of 0.006 m/z or 10.0 ppm, (4) Chromatogram deconvolution using the local minimum search algorithm with a 70% chromatographic threshold, 0.05 min minimum RT range, 5% minimum relative height, 1200 minimum absolute height, a minimum ration of peak top/edge of 1.2 and a peak duration range of 0.08 - 5.0, (5), Isotopic peak grouper with a m/z tolerance of 5.0 ppm, RT tolerance of 0.05 min, maximum charge of 2 and with the most intense isotope set as the representative isotope, (6) Peak filter with minimum 12 data points, a FWHM between 0.0 and 0.2, tailing factor between 0.45 and 2.22 and asymmetry factor between 0.40 and 2.50, (7) Join aligner with a m/z tolerance of 0.009 or 10.0 ppm and a weight for of 2, a RT tolerance of 0.1 min and a weight of 1 and with no requirement of charge state or ID and no comparison of isotope pattern, (8) Peak list row filter with a minimum of 10% of the samples (10) Gap filling using the same RT and m/z range gap filler algorithm with an m/z tolerance of 0.009 m/z or 11.0 ppm, (11) Identification of lipids using a custom database search with an m/z tolerance of 0.009 m/z or 10.0 ppm and a RT tolerance of 0.1 min, and (12) Normalization using internal standards PE(17:0/17:0), SM(d18:1/17:0), Cer(d18:1/17:0), LPC(17:0), TG(17:0/17:0/17:0) and PC(16:0/d30/18:1)) for identified lipids and closest ISTD for the unknown lipids followed by calculation of the concentrations based on lipid-class concentration curves.

An aliquot of each sample was collected and pooled and used as quality control sample, together with NIST SRM1950 reference plasma sample, an in-house pooled serum sample.

Analyses of polar metabolites by GC-TOFMS

Serum samples were randomized and sample preparation was done as described previously[48, 49]. In summary, 400 µL of MeOH containing ISTDs (heptadecanoic acid, deuterium-labeled DL-valine, deuterium-labeled succinic acid, and deuterium-labeled glutamic acid, c= 1 µg/ml) was added to 30 µl of the serum samples which were vortex mixed and incubated on ice for 30 min after which they were centrifuged (9400 × g, 3 min) and 350 µL of the supernatant was collected after centrifugation. The solvent was evaporated to dryness and 25 µL of MOX reagent was added and the sample was incubated for 60 min at 45 °C. 25 µL of MSTFA was added and after 60 min incubation at 45 °C 25 µL of the retention index standard mixture (n-alkanes, c=10 µg/ml) was added.

The analyses were carried out on an Agilent 7890B GC coupled to 7200 Q-TOF MS. Injection volume was 1 µL with 100:1 cold solvent split on PTV at 70 °C, heating to 300 °C at 120 °C/minute. Column: Zebron ZB-SemiVolatiles. Length: 20m, I.D. 0.18mm, film thickness: 0.18 µm. With initial Helium flow 1.2 mL/min, increasing to 2.4 mL/min after 16 mins. Oven temperature program: 50 °C (5 min), then to 270°C at 20 °C/min and then to 300 °C at 40 °C/min (5 min). EI source: 250 °C, 70 eV electron energy, 35µA emission, solvent delay 3 min. Mass range 55 to 650 amu, acquisition rate 5 spectra/s, acquisition time 200 ms/spectrum. Quad at 150 °C, 1.5 mL/min N_2 collision flow, aux-2 temperature: 280 °C.

Calibration curves were constructed using alanine, citric acid, fumaric acid, glutamic acid, glycine, lactic acid, malic acid, 2-hydroxybutyric acid, 3-hydroxybutyric acid, linoleic acid, oleic acid, palmitic acid, stearic acid, cholesterol, fructose, glutamine, indole-3-propionic acid, isoleucine, leucine, proline, succinic acid, valine, asparagine, aspartic acid, arachidonic acid, glycerol-3-phosphate, lysine,

methionine, ornithine, phenylalanine, serine and threonine purchased from Sigma-Aldrich (St. Louis, MO, USA) at concentration range of 0.1 to 80 μg/ml. An aliquot of each sample was collected and pooled and used as quality control samples, together with a NIST SRM 1950 serum sample and an in-house pooled serum sample. Relative standard deviations (% RSDs) of the metabolite concentrations in control serum samples showed % RSDs within accepted analytical limits at averages of 12.3% and 19.6% for the maternal and cord blood serum samples, respectively, and 7.2% for serum samples from NOD mice.

Data transformation and descriptive statistical analysis

Spreadsheets containing concentration data were converted to .csv format for loading into the R statistical programming language[50]. For all datasets, the following transformations were carried out:

1. NA values in the data were replaced with zeroes.
2. The aforementioned zeroes were then replaced with imputed half-minimums (for each variable, the minimum value was found, and half of this value was used)
3. All values were log2 transformed.
4. Each variable was scaled to zero mean and unit variance.

Total PFAS exposure in pregnant mothers was assessed as a simple sum of exposure to all measured PFAS. Mothers and matching children were then sorted into quartiles of this total maternal PFAS exposure. Analysis by both ANOVA and Tukey's honest significant difference (TukeyHSD) were carried out on all lipids and metabolites in the infants' cord blood, grouping these into the aforementioned maternal PFAS exposure quartiles to reveal any significant changes in their level as exposure increased. To visualize this, the R beanplot package (version 1.2)[51] was used to show both the changes in the means across exposure quartiles, and the densities of samples in each quartile.

Two-way analysis of variance was performed with factors HLA risk and PFAS exposure) and their interactions in MATLAB R2017b (Mathworks, Inc., Natick, MA, USA) using Statistical Toolbox.

Clustering

All metabolomics datasets were then analyzed using the mclust R package (version 5.4.1)[25] to assign variables (lipids / metabolites) from each dataset to separate clusters. Here, mclust attempts to fit various model types and assesses their performance using the Bayesian Information Criterion (BIC). The highest BIC achieved by mclust for each dataset was used to determine both the model type and the number of clusters into which the variables should be divided. The variables in each dataset were thusly given numbers to denote their cluster membership. Plots demonstrating the distribution of BICs for each dataset are given in supplementary data.

For each sample in each dataset, cluster variables were then generated. For each dataset, the number of clusters *k* found by mclust equals the number of cluster variables generated. Each cluster variable is the mean value of the lipids / metabolites that make up that cluster, meaning that samples in that dataset are represented now only by *k* values. These cluster variables were given acronyms indicating the dataset from which they were generated (Mothers' blood Lipids Cluster – MLC, Mothers' polar Metabolites Cluster - MMC, Cord blood Lipids Cluster - CLC, Cord blood polar Metabolites Cluster – CMC).

These cluster variable acronyms had their cluster numbers (1-*k* for each dataset) appended to them to form their final labels. Assignment of individual lipids / metabolites to each cluster variable is given for each dataset in supplementary files, along with total membership counts in each cluster. PFAS compounds were not clustered in this manner and so retain their names.

Partial correlation network analysis

With dataset dimensionality reduced to the aforementioned cluster variables, partial correlation analysis was employed, taking all cluster variables into account, along with clinical values, simultaneously. Pairwise Spearman correlations between all of the aforementioned variables were calculated. To subsequently visualize this, the corrplot R package (version 0.84) was used. For legibility of figures, the

colors of these plots generated by corrplot were limited to either solid orange or blue for positive or inverse correlations respectively, with correlation strength represented purely through the size of the filled circles for each pairwise correlation.

For network analysis and representation based on the generated partial correlations, the qpNrr() function from the qpgraph R package (version 2.16.0)[26] was run with default parameters to estimate non-rejection rates (NRRs) of the aforementioned correlation matrix of all datasets' cluster variables and clinical features. This is a means for rejecting spurious correlations. The obtained NRR matrix was then filtered at various thresholds (0.1 to 1, with an increment of 0.1) to provide the edges for network graphing. The distribution of NRRs was also visualized as a histogram to assist with choosing an appropriate cut-off threshold for retaining plausible, and rejecting likely spurious, correlations. These are given in supplementary figures. Based on the distribution of NRRs and observed network topology of the generated networks, a cut-off of 0.5 was deemed appropriate.

The Rgraphviz R package (version 2.26.0)[52] was used to generate network topography plots. Node and edge properties for these network graphs were generated in a custom fashion. Edges were colored by the directionality of the relationship between the nodes that they connect. Edge width was plotted as a function of the strength of the Spearman correlation between the two variables that the edge connects. Nodes were colored and shaped purely for clarity and to group like variables (PFAS, clinical variables, cluster variables) and sample sources (mothers, infants) together. Network layout is generated by the Rgraphviz package itself, and layout was set to the "neato" parameter to balance clarity and compactness.

For both the final correlation plot and network figure, values were used only from those sample identifiers uniquely represented in all four datasets (mothers' blood lipids, mothers' polar metabolites, cord blood lipids, cord blood polar metabolites), totaling (n = 224 samples, n = 59 variables).

Data accessibility

The lipidomics datasets and the clinical metadata generated in this study were submitted to MetaboLights[53] under accession number (MTBLS875). The relevant clinical metadata from the EDIA study was linked to the lipidomics dataset using the ISA-creator package from MetaboLights.

Ethical approval and informed consent

The Ethical Committee of the Pirkanmaa Hospital District has approved the EDIA study. The parents gave their written informed consent to their own participation and to the participation of their newborn infant in the study. The conduct of the EDIA study conforms to the standards of the Declaration of Helsinki.

Acknowledgments

The EDIA study was supported by the National Institute of Diabetes and Digestive and Kidney Diseases (NIDDK), National Institutes of Health (No. 1DP3DK094338-01 to M.K.), the Academy of Finland Centre of Excellence in Molecular Systems Immunology and Physiology Research 2012-17, No. 250114 to M.K. and M.O.), and the Medical Research Funds, Tampere and Helsinki University Hospitals (to M.K.). The current work was also supported by the Juvenile Diabetes Research Foundation (2-SRA-2016-341-S-B to M.K., T.H. and M.O., 2-SRA-2016-289-S-B to M.O.), Academy of Finland (No. 292568 to M.O.), Vetenskapsrådet (No. 2016-05176 to T.H.), and the Knowledge Foundation (to T.H.).

Author contributions

T.H. initially proposed the study of PFAS exposure in the mother-infant study (EDIA), while M.O. proposed the follow-up metabolomics studies in NOD mice. T.H., M.O. and M.K. initiated and designed the study. M.K. is the principal investigator of the mother-infant study. M.O. supervised data analysis and integration, and together with T.H. did the primary interpretation of analytical outcomes. A.M., M.O., S.L. and T.H. analyzed the data. T.H. supervised metabolomic and PFAS analyses. T.S., D.G., C.C.,

D.D. performed sample analyses. J.B., H.D. and U.C.N. conducted the studies in NOD mice, while H.F.B. and K.Z. assembled the internal relationship of chemicals in the feed for POP-exposure. H.S. contributed clinical research in the mother-infant cohort. J.I. performed genetic analyses in the mother-infant study. S.M.V. performed the study of dietary intake in the mother-child study. A.M., M.O. and T.H. wrote the first version of the paper. All authors approved the final version.

REFERENCES

1. Atkinson MA, Eisenbarth GS, Michels AW. Type 1 diabetes. *Lancet* **383**, 69-82 (2014).
2. Noble JA, Erlich HA. Genetics of type 1 diabetes. *Cold Spring Harb Perspect Med* **2**, a007732 (2012).
3. Achenbach P, Bonifacio E, Koczwara K, Ziegler AG. Natural history of type 1 diabetes. *Diabetes* **54 Suppl 2**, S25-31 (2005).
4. Knip M, Veijola R, Virtanen SM, Hyöty H, Vaarala O, Åkerblom HK. Environmental triggers and determinants of type 1 diabetes. *Diabetes* **54**, S125-136 (2005).
5. Orešič M, *et al.* Dysregulation of lipid and amino acid metabolism precedes islet autoimmunity in children who later progress to type 1 diabetes. *J Exp Med* **205**, 2975-2984 (2008).
6. Lamichhane S, *et al.* Dynamics of Plasma Lipidome in Progression to Islet Autoimmunity and Type 1 Diabetes - Type 1 Diabetes Prediction and Prevention Study (DIPP). *Sci Rep* **8**, 10635 (2018).
7. Orešič M, *et al.* Cord serum lipidome in prediction of islet autoimmunity and type 1 diabetes. *Diabetes* **62**, 3268-3274 (2013).
8. La Torre D, *et al.* Decreased cord-blood phospholipids in young age-at-onset type 1 diabetes. *Diabetes* **62**, 3951-3956 (2013).
9. Velagapudi VR, *et al.* The gut microbiota modulates host energy and lipid metabolism in mice. *J Lipid Res* **51**, 1101-1112 (2010).
10. Kostic AD, *et al.* The dynamics of the human infant gut microbiome in development and in progression toward type 1 diabetes. *Cell Host Microbe* **17**, 260-273 (2015).
11. Vatanen T, *et al.* The human gut microbiome in early-onset type 1 diabetes from the TEDDY study. *Nature* **562**, 589-594 (2018).
12. Patterson CC, Dahlquist GG, Gyürüs E, Green A, Soltész G. Incidence trends for childhood type 1 diabetes in Europe during 1989-2003 and predicted new cases 2005-20: a multicentre prospective registration study. *Lancet* **373**, 2027-2033 (2009).
13. Berhan Y, Waernbaum I, Lind T, Möllsten A, Dahlquist G, for the Swedish Childhood Diabetes Study G. Thirty Years of Prospective Nationwide Incidence of Childhood Type 1 Diabetes: The Accelerating Increase by Time Tends to Level Off in Sweden. *Diabetes* **60**, 577-581 (2011).
14. Harjutsalo V, Sund R, Knip M, Groop PH. Incidence of type 1 diabetes in Finland. *JAMA* **310**, 427-428 (2013).
15. Kaikkonen R, *et al.* Health and well-being inequalities among children and their families. National Institute for Health and Wellfare. Report 16/2012 (2012).
16. Wang T, Vestergren R, Herzke D, Yu J, Cousins IT. Levels, Isomer Profiles, and Estimated Riverine Mass Discharges of Perfluoroalkyl Acids and Fluorinated Alternatives at the Mouths of Chinese Rivers. *Environ Sci Technol* **50**, 11584-11592 (2016).
17. Gebbink WA, Glynn A, Berger U. Temporal changes (1997-2012) of perfluoroalkyl acids and selected precursors (including isomers) in Swedish human serum. *Environ Pollut* **199**, 166-173 (2015).
18. Bjerregaard-Olesen C, *et al.* Time trends of perfluorinated alkyl acids in serum from Danish pregnant women 2008-2013. *Environ Int* **91**, 14-21 (2016).
19. Croes K, *et al.* Persistent organic pollutants (POPs) in human milk: a biomonitoring study in rural areas of Flanders (Belgium). *Chemosphere* **89**, 988-994 (2012).

20. Bodin J, Stene LC, Nygaard UC. Can exposure to environmental chemicals increase the risk of diabetes type 1 development? *Biomed Res Int* **2015**, 208947 (2015).

21. Liu S, Yin N, Faiola F. PFOA and PFOS Disrupt the Generation of Human Pancreatic Progenitor Cells. *Environmental Science & Technology Letters* **5**, 237-242 (2018).

22. Bodin J, Groeng EC, Andreassen M, Dirven H, Nygaard UC. Exposure to perfluoroundecanoic acid (PFUnDA) accelerates insulitis development in a mouse model of type 1 diabetes. *Toxicol Rep* **3**, 664-672 (2016).

23. Predieri B, Iughetti L, Guerranti C, Bruzzi P, Perra G, Focardi SE. High Levels of Perfluorooctane Sulfonate in Children at the Onset of Diabetes. *Int J Endocrinol* **2015**, 234358 (2015).

24. Land M, *et al.* What is the effect of phasing out long-chain per- and polyfluoroalkyl substances on the concentrations of perfluoroalkyl acids and their precursors in the environment? A systematic review. *Environmental Evidence* **7**, 4 (2018).

25. Scrucca L, Fop M, Murphy TB, Raftery AE. mclust 5: Clustering, Classification and Density Estimation Using Gaussian Finite Mixture Models. *R J* **8**, 289-317 (2016).

26. Castelo R, Roverato A. Reverse engineering molecular regulatory networks from microarray data with qp-graphs. *J Comp Biol* **16**, 213-227 (2009).

27. Averina M, Brox J, Huber S, Furberg AS. Perfluoroalkyl substances in adolescents in northern Norway: Lifestyle and dietary predictors. The Tromso study, Fit Futures 1. *Environ Int* **114**, 123-130 (2018).

28. Ottestad I, *et al.* Fish oil supplementation alters the plasma lipidomic profile and increases long-chain PUFAs of phospholipids and triglycerides in healthy subjects. *PLoS One* **7**, e42550 (2012).

29. Salihovic S, *et al.* Identification of metabolic profiles associated with human exposure to perfluoroalkyl substances. *J Expo Sci Environ Epidemiol* **29**, 196-205 (2019).

30. Berntsen HF, *et al.* Decreased macrophage phagocytic function due to xenobiotic exposures in vitro, difference in sensitivity between various macrophage models. *Food Chem Toxicol* **112**, 86-96 (2018).

31. Gebbink WA, Glynn A, Darnerud PO, Berger U. Perfluoroalkyl acids and their precursors in Swedish food: The relative importance of direct and indirect dietary exposure. *Environ Pollut* **198**, 108-115 (2015).

32. Berntsen HF, Berg V, Thomsen C, Ropstad E, Zimmer KE. The design of an environmentally relevant mixture of persistent organic pollutants for use in in vivo and in vitro studies. *J Toxicol Environ Health A* **80**, 1002-1016 (2017).

33. Haug LS, Thomsen C, Becher G. Time trends and the influence of age and gender on serum concentrations of perfluorinated compounds in archived human samples. *Environ Sci Technol* **43**, 2131-2136 (2009).

34. Hart K, *et al.* Time trends and transplacental transfer of perfluorinated compounds in melon-headed whales stranded along the Japanese coast in 1982, 2001/2002, and 2006. *Environ Sci Technol* **42**, 7132-7137 (2008).

35. Winkens K, Vestergren R, Berger U, Cousins IT. Early life exposure to per- and polyfluoroalkyl substances (PFASs): A critical review. *Emerging Contaminants* **3**, 55-68 (2017).

36. Kim S, *et al.* Trans-placental transfer of thirteen perfluorinated compounds and relations with fetal thyroid hormones. *Environ Sci Technol* **45**, 7465-7472 (2011).

37. Mamsen LS, *et al.* Concentration of perfluorinated compounds and cotinine in human foetal organs, placenta, and maternal plasma. *Sci Total Environ* **596-597**, 97-105 (2017).

38. DeWitt JC, *et al.* Immunotoxicity of perfluorooctanoic acid and perfluorooctane sulfonate and the role of peroxisome proliferator-activated receptor alpha. *Crit Rev Toxicol* **39**, 76-94 (2009).

39. Holm LJ, *et al.* Abnormal islet sphingolipid metabolism in type 1 diabetes. *Diabetologia* **61**, 1650-1661 (2018).

40. Hermann R, *et al.* HLA DR-DQ-encoded genetic determinants of childhood-onset type 1 diabetes in Finland: an analysis of 622 nuclear families. *Tissue Antigens* **62**, 162-169 (2003).

41. Ilonen J, *et al.* Genetic susceptibility to type 1 diabetes in childhood - estimation of HLA class II associated disease risk and class II effect in various phases of islet autoimmunity. *Pediatr Diabetes* **17 Suppl 22**, 8-16 (2016).

42. Erkkola M, Karppinen M, Javanainen J, Rasanen L, Knip M, Virtanen SM. Validity and reproducibility of a food frequency questionnaire for pregnant Finnish women. *Am J Epidemiol* **154**, 466-476 (2001).

43. National Institute of Health and Welfare. National Food Composition Database in Finland (https://fineli.fi/fineli/en/index).

44. Salihovic S, Karrman A, Lindstrom G, Lind PM, Lind L, van Bavel B. A rapid method for the determination of perfluoroalkyl substances including structural isomers of perfluorooctane sulfonic acid in human serum using 96-well plates and column-switching ultra-high performance liquid chromatography tandem mass spectrometry. *J Chromatogr A* **1305**, 164-170 (2013).

45. Pedersen HK, *et al.* A computational framework to integrate high-throughput '-omics' datasets for the identification of potential mechanistic links. *Nat Protoc* **13**, 2781-2800 (2018).

46. Nygren H, Seppanen-Laakso T, Castillo S, Hyotylainen T, Oresic M. Liquid chromatography-mass spectrometry (LC-MS)-based lipidomics for studies of body fluids and tissues. *Methods Mol Biol* **708**, 247-257 (2011).

47. Pluskal T, Castillo S, Villar-Briones A, Oresic M. MZmine 2: modular framework for processing, visualizing, and analyzing mass spectrometry-based molecular profile data. *BMC Bioinformatics* **11**, 395 (2010).

48. Hartonen M, Mattila I, Ruskeepää A-L, Orešič M, Hyötyläinen T. Characterization of cerebrospinal fluid by comprehensive two-dimensional gas chromatography coupled to time-of-flight mass spectrometry. *J Chromatogr A* **1293**, 142-149 (2013).

49. Castillo S, Mattila I, Miettinen J, Orešič M, Hyotylainen T. Data analysis tool for comprehensive two-dimensional gas chromatography/time-of-flight mass spectrometry. *Anal Chem* **83**, 3058-3067 (2011).

50. R Development Core Team. R: A language and environment for statistical computing. R Foundation for Statistical Computing (2018).

51. Kampstra P. Beanplot: a boxplot alternative for visual comparison of distributions. *J Stat Soft* **28**, 1-9 (2008).

52. Hansen KD, *et al.* Rgraphviz: Provides plotting capabilities for R graph objects. R package version 2.27.0. (2018).

53. Kale NS, *et al.* MetaboLights: An Open-Access Database Repository for Metabolomics Data. *Curr Protoc Bioinformatics* **53**, 14 13 11-18 (2016).

Supplementary Figure 1. Correlation plot of PFAS exposure, metabolite cluster and demographic data in the mother-infant cohort.

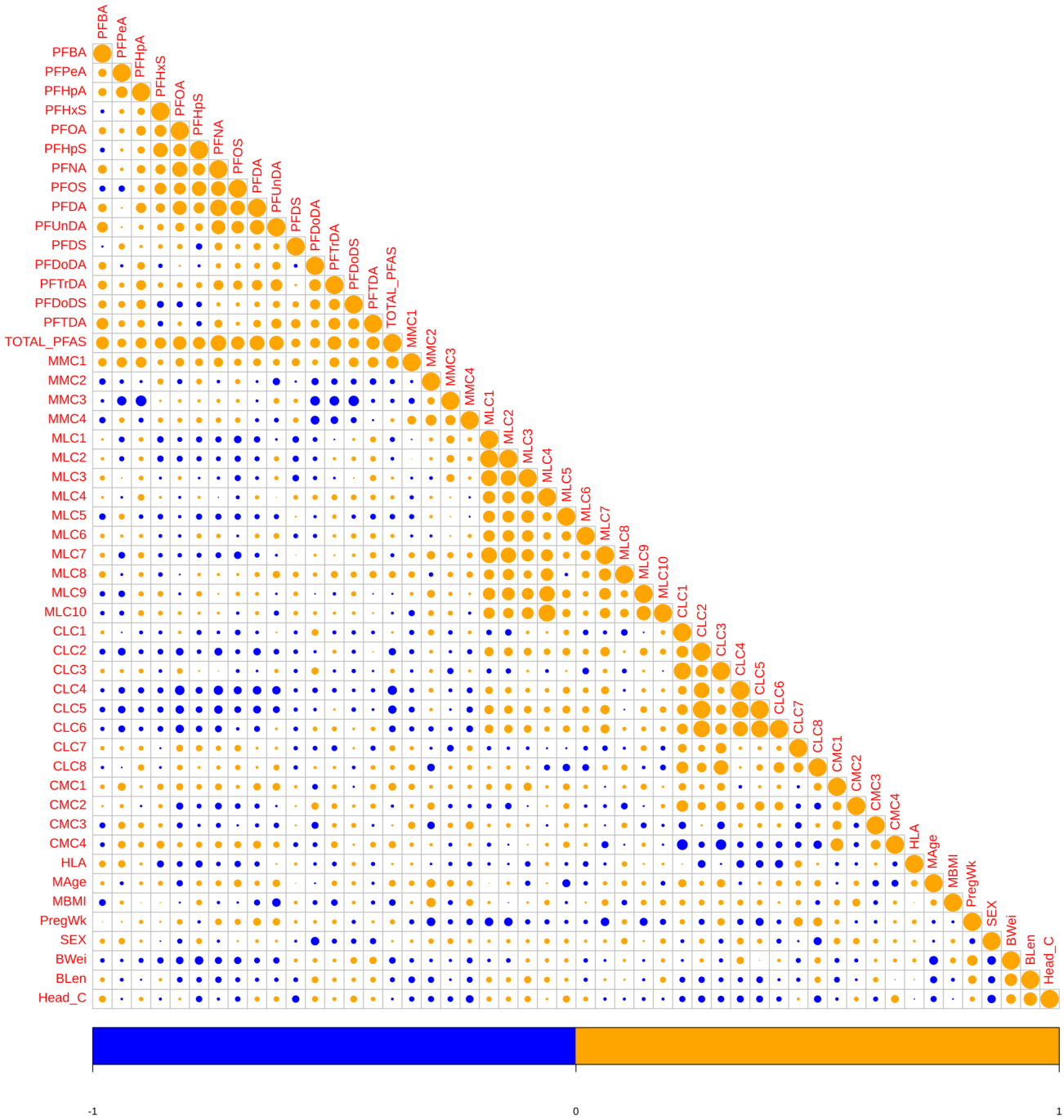

Supplementary Figure 2. Correlation of PFAS exposure and dietary factors during pregnancy.

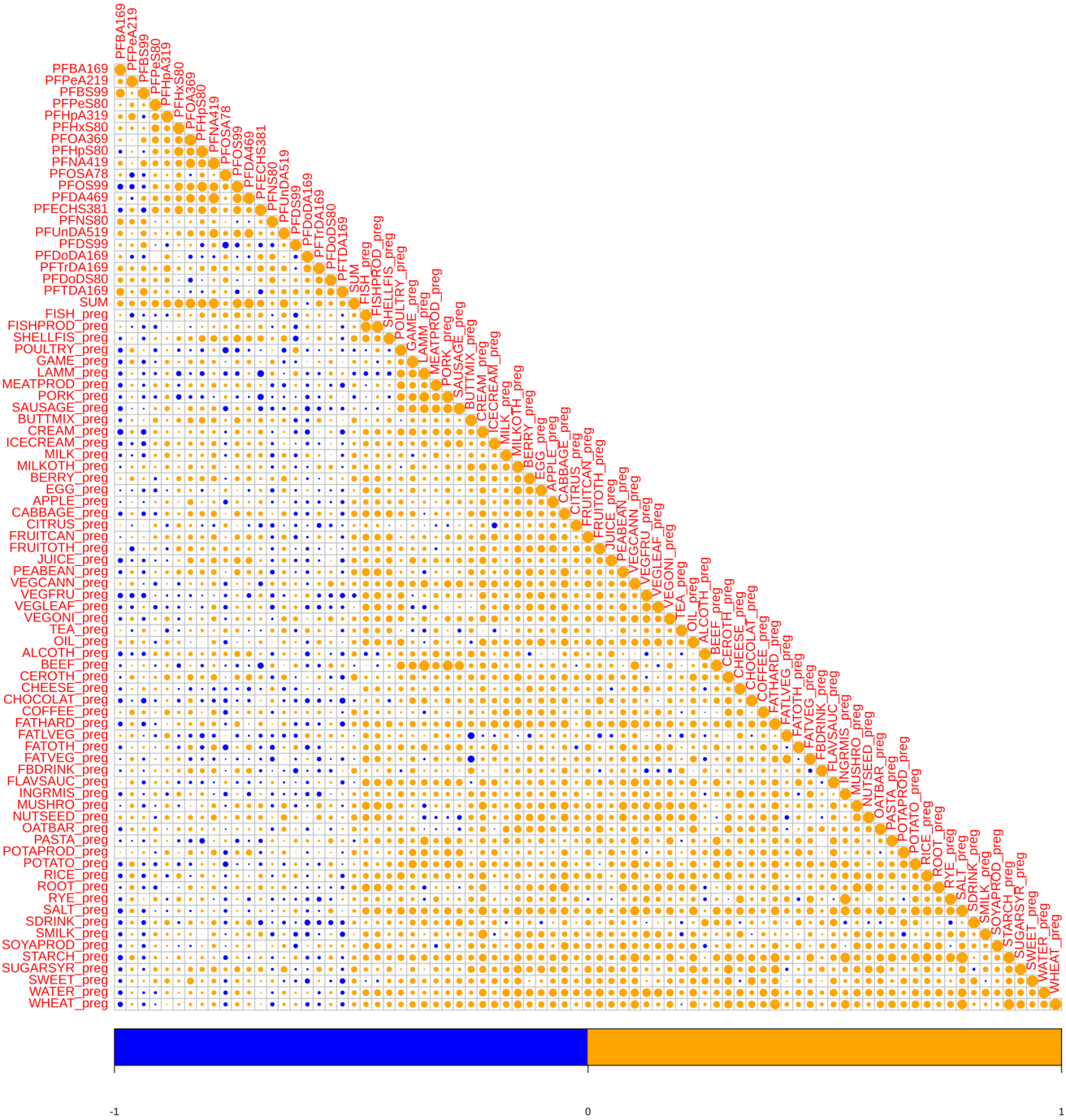

Supplementary Table 1. Demographic data of the study population.

Parameter	Median (range)
Maternal age (years)	31.5 (18.5-45.8)
Pre-pregnancy BMI (kg/m2)	23.4 (16.9-45.7)
Gestational age (weeks)	40 (35.7-42.4)
Gender of the baby (%)	50/50
Birth weight (g)	3530 (1670-4720)
Head circumference (cm)	35 (31-8.8)
Asp. points at birth (1 min, 5 min)	9 (4-10) / 9 (7-10)
Smoking status* (nonsmokers/smokers)	94.5/5.5
Delivery type: vaginal/cesarean (%)*	87/13
Weight at 12 months (median (min-max) kg)**	9.9 (8.1-13.2)
Head circumference at 12 months (median (min-max) cm)**	35 (31-38.5)
HLA risk (low/increased, %)***	56/44

*For a subgroup of 116 pairs
**For a subgroup of 44 infants
***Genotypes where HLA-(DR3)-DQA1*05-DQB*02 and/or DRB1*04:01/2/4/5-DQA1*03-DQB1*03:02 are present with each other, homozygous or heterozygous with a neutral haplotype were classified as increased risk and all other genotypes as low risk.

Supplementary Table 2. List of PFAS measured in the pregnant mothers. Abbreviations: Q, quartile; IQR, inter-quartile range.

Full name	Abbreviation	Detection rate (%)	Median (ng/mL)	Q1	Q3	IQR
Potassium 11-chloroeicosafluoro-3-oxaundecane-1-sulfonate	11ClPF3OUdS	0	-			
4:2 fluorotelomer sulfonate	4:2 FTSA	1	0.075	0.075	0.12	0.044
6:2 fluorotelomer sulfonate	6:2 FTSA	7	0.18	0.14	0.28	0.13
8:2 fluorotelomer sulfonate	8:2 FTSA	1	0.047	0.049	0.055	0.006
Potassium 9-chlorohexadecafluoro-3-oxanonane-1-sulfonate	9ClPF3ONS	0	-			
Perfluorobutanoic acid	PFBA	17	0.37	0.29	0.43	0.14
Perfluorobutane sulfonate	PFBS	1	0.059	0.061	0.064	0.003
Perfluorodecanoic acid	PFDA	94	0.19	0.14	0.25	0.11
Perfluorododecanoic acid	PFDoDA	5	0.083	0.062	0.12	0.056
Perfluorododecane sulfonate	PFDoDS	6	0.12	0.11	0.2	0.093
Perfluorodecane sulfonate	PFDS	8	0.056	0.046	0.08	0.029
Potassium Perfluoro-4-ethylcyclohexanesulfonate	PFECHS	0		0.061	0.061	0
Perfluoroheptanoic acid	PFHpA	21	0.12	0.04	0.19	0.15
Perfluoroheptane sulfonate	PFHpS	34	0.058	0.048	0.074	0.027
Perfluorohexane sulfonate	PFHxS	99	0.33	0.27	0.43	0.16
Perfluorononanoic acid	PFNA	100	0.39	0.28	0.536	0.25
Perfluorononane sulfonate	PFNS	0	0.03	0.06	0.06	0
Perfluorooctanoic acid	PFOA	100	1.02	0.68	1.41	0.72
Linear-Perfluorooctane sulfonate	L-PFOS	100	1.38	0.97	1.86	0.89
Perfluorooctane sulfonamide	PFOSA	0	-			
Perfluoropentanoic acid	PFPeA	12	0.15	0.13	0.21	0.08
Perfluoro pentane sulfonate	PFPeS	1	0.04	0.04	0.06	0.015
Perfluorotetradecanoic acid	PFTDA	12	0.32	0.1	0.75	0.65
Perfluorotridecanoic acid	PFTrDA	12	0.11	0.06	0.2	0.14
Perfluoroundecanoic acid	PFUnDA	55	0.27	0.23	0.34	0.1

Supplementary Table 3. Description of the lipid and polar metabolite clusters from mothers.

Cluster	Description	Most abundant lipids
MLC1	Major phospholipids, one CE	CE(16:0), PC(34:2), PC(16:0/18:1), PC(36:2)
MLC2	Phospholipids, cholesterol ester	CE(18:1), PC(32:1), PC(36:3), PC(36:5)
MLC3	Ceramides	Cer(d18:1/24:1), Cer(d18:1/24:0)
MLC4	TGs with C50-52, mainly unsaturated, mono-unsaturated	TG(18:1/18:1/16:0), TG(18:2/18:1/16:0) TG(14:0/18:1/18:1)
MLC5	LLPCs	LPC(18:0), LPC(18:1), LPC(18:2)
MLC6	Ether phospholipids	PE(O-16:0/22:6) , PC(O-38:5)
MLC7	PEs	PE(38:6), PE(38:4), PE(16:0/18:1)
MLC8	Small TGs (C<50) with SFAs	TG(14:0/16:0/18:1), TG(18:1/12:0/18:1), TG(16:0/16:0/16:0)
MLC9	Large TGs (>54) with PUFAs	TG(18:2/22:5/16:0), TG(16:0/22:5/18:1(, TG(54:6)
MLC10	Medium TGs with PUFA	TG(18:1/18:1/18:1),TG(18:2/18:1/18:1) TG(18:1/18:2/18:2)
MMC1	Amino acids, free cholesterol, saturated free fatty acids	Alanine, Decanoic acid, Lactic acid, Octanoic acid, Palmitic acid, Cholesterol
MMC2	Amino acids and hydroxy acids	2-and 3-hydroxybutyric acids, Glutamic acid, Glycine, Serine
MMC3	Main free fatty acids, amino acids	Glutamine, Linoleic acid, Oleic acid, Stearic acid
MMC4	Branched-chain amino acids	Isoleucine, Leucine, Valine

Supplementary Table 4. Lipid and polar metabolite cluster description from newborn infants.

Cluster	General description	Main lipids
CLC1	Cholesterol esters, DGs, TGs	CE(18:1), CE(16:0), CE(20:4), TG(18:2/18:1/18:1), DG(36:2), TG(18:1/18:1/18:1)
CLC2	Phospholipids with PUFAs, SMs	SM(42:1), PC(38:4), PC(38:6), PC(40:6), PC(18:0/18:0)
CLC3	Main TGs	TG(18:2/18:1/16:0), TG(14:0/18:1/18:1), TG(16:0/18:2/18:2)
CLC4	LPCs	LPC(18:0), LPC(18:1),LPC(20:4)
CLC5	Abundant PCs and SMs	SM(42:2), PC(18:0/18:1), SM(42:3), SM(38:1)
CLC6	Odd-chain PCs	PC(35:1), PC(33:1), PC(35:2)
CLC7	Phospholipids with PUFAs	PC(36:3), PC(40:7), PC(O-40:6)
CLC8	Odd-chain TGs	TG(45:0), TG(47:0), TG(47:1), TG(47:2)
CMC1	Amino acids, dicarboxylic and hydroxyl acids	Alanine, Glycine, Glutamic acid, Fumaric acid Malic acid, Citric acid, Lactic acid
CMC2	2- and 3-butyric acids, main free fatty acids	2-Hydroxybutyric acid, 3-Hydroxybutyric acid Palmitic acid, Linoleic acid, Oleic acid, Stearic acid
CMC3	BCAAs, sugar derivatives	Valine, Leucine, Isoleucine, Proline, Succinic acid, Glutamine, Fructose, Indole-3-propionic acid, Cholesterol
CMC4	Amino acids	Serine, Threonine, Methionine, Aspartic acid Phenylalanine, Asparagine, Glycerol-3-phosphate, Ornithine, Lysine

Supplementary Table 5. Associations of PFAS exposure (quartiles) and cord serum metabolite clusters (CLC, CMC).

	ANOVA	2-1	3-1	4-1	3-2	4-2	4-3
CLC1	0.5208	0.9999	0.8584	0.6381	0.8240	0.5893	0.9814
CLC2	0.1621	0.7295	0.3363	0.1435	0.9074	0.6743	0.9722
CLC3	0.9632	0.9956	0.9919	0.9996	0.9546	0.9863	0.9979
CLC4	**0.0047**	0.1514	**0.0412**	**0.0032**	0.9346	0.4985	0.8592
CLC5	0.0855	0.3977	0.2369	0.0673	0.9854	0.7939	0.9446
CLC6	0.2578	1.0000	0.7400	0.3577	0.7143	0.3302	0.9296
CLC7	0.1763	0.5275	0.3669	0.1458	0.9910	0.8573	0.9624
CLC8	0.4867	0.4701	0.9724	0.7307	0.7511	0.9766	0.9358
CMC1	0.1268	0.8992	0.8410	0.0948	0.9991	0.3638	0.4478
CMC2	0.8538	0.9993	0.9622	0.8566	0.9836	0.9080	0.9902
CMC3	0.0879	0.1189	0.3897	0.1187	0.9210	1.0000	0.9229
CMC4	**0.0011**	0.5044	0.9410	**0.0011**	0.8457	0.0838	**0.0087**

Supplementary Table 6. Cord blood lipids associated with the level of maternal exposure.

	Tukey HSD Quartile Comparison Group						
Lipid	**ANOVA**	**2-1**	**3-1**	**4-1**	**3-2**	**4-2**	**4-3**
LPC(20:4)	**0.015**	0.159	0.178	**0.008**	1.000	0.682	0.648
LPC(18:1)	**0.021**	0.762	0.242	**0.015**	0.810	0.183	0.671
LPC(22:6)	**0.024**	0.308	0.119	**0.017**	0.961	0.602	0.877
LPC(20:3)	**0.032**	0.444	0.202	**0.020**	0.964	0.486	0.780
LPC(18:2)	**0.037**	0.675	0.276	**0.024**	0.908	0.312	0.717
SM(d38:1)	**0.043**	0.326	0.199	**0.029**	0.993	0.701	0.852
PC(40:8)	0.064	0.327	0.520	**0.040**	0.988	0.765	0.564
SM(d36:0)*	0.057	0.600	0.235	**0.041**	0.918	0.491	0.867
SM(d36:0)*	0.070	0.417	0.466	**0.041**	1.000	0.678	0.627
LPC(22:5)	**0.041**	0.508	0.089	**0.048**	0.771	0.619	0.994
PC(O-38:4)	**0.026**	0.476	0.499	0.782	0.026	0.085	0.968
Methionine	**0.026**	0.087	0.517	**0.025**	0.764	0.969	0.479
Aspartic acid	**0.042**	0.072	0.269	0.056	0.927	1.000	0.901
Phenylalanine	**0.048**	0.057	0.837	0.163	0.335	0.962	0.616

*These two lipids share the same carbon number, but due to different retention time in lipidomic analysis, they are considered different molecular species, likely due to different sphingosine and fatty acyl groups adding up to the same carbon number.

Supplementary Table 7. Associations previously reported lipid clusters[7] and PFAS exposure.

	LC2	LC3	LC4	LC5	LC6	LC7	LC8	LC9	LC10
PFOS	0.197	**0.039**	0.862	0.553	0.347	0.061	0.325	0.543	0.963
PFOA	**0.095**	**0.013**	0.067	0.488	0.208	**0.034**	0.111	0.397	0.522
PFUnDA	0.066	0.064	0.867	0.645	0.247	**0.046**	0.624	0.980	0.936
PfHPeA	0.230	**0.046**	0.425	0.238	0.442	0.077	0.100	0.170	0.209
PFPeA	**0.013**	0.180	**0.034**	0.304	**0.004**	**0.011**	0.109	0.468	0.736
PFNA	**0.002**	**0.001**	0.110	0.791	**0.011**	**0.001**	0.519	0.788	0.922
PFDA	**0.049**	**0.007**	0.397	0.891	0.052	**0.020**	0.496	0.546	0.492
SUM	**0.024**	**0.027**	0.120	0.919	0.076	**0.009**	0.945	0.897	0.999

Supplementary Table 8. Associations of previously reported T1D-associated lipids with PFAS exposure.

LIPID	SUM	PFBA	PFDA	PFNA	PFOA	PFOS	PFUnDA
SM(d18:1/16:0)	**0.047**	0.150	**0.014**	**0.003**	**0.080**	0.061	**0.043**
PC(p32:0)	0.053	0.182	0.116	**0.014**	0.150	0.090	0.103
SM(d18:1/18:0)	**0.016**	0.185	**0.015**	**0.001**	**0.027**	**0.018**	**0.036**
PC(16:0/16:1)	**0.028**	0.313	0.184	**0.018**	**0.023**	0.468	0.267
PC(16:0/18:3)	0.069	**0.029**	0.134	**0.010**	0.104	0.120	0.159
SM(d18:1/20:0)	**0.022**	0.232	**0.047**	**0.008**	0.065	**0.024**	0.099
PC(16:0/18:1)	0.053	0.280	0.134	**0.015**	0.079	0.323	0.196
SM(d18:0/20:0)	**0.015**	0.452	**0.033**	**0.005**	**0.037**	**0.040**	0.186
SM(d18:2/24:1)	0.055	0.167	0.162	**0.010**	0.145	0.075	0.112
PC(18:0/20:3)	0.079	0.322	0.038	**0.010**	0.251	0.119	0.107
SM(d18:1/24:1)	0.079	0.226	0.184	**0.020**	0.179	0.053	0.127
SM(18:0/24:2)	**0.041**	0.416	0.091	**0.011**	0.146	0.071	0.297
SM(d18:0/24:1)	**0.045**	0.424	0.156	**0.022**	0.150	0.104	0.362
PC(18:0/18:1)	**0.024**	0.178	0.097	**0.011**	0.066	0.140	0.089

Supplementary Table 9. Two-way ANOVA analysis for cord serum lipids affected by PFAS exposure (**Supplementary Table 6**), with samples assigned according to HLA-associated T1D risk (strongly protective / neutral *vs.* mild / high risk) and prenatal total PFAS exposure (quartiles 1 & 2 *vs.* 3 & 4). p-values are shown.

Lipid	**HLA**	**PFAS**	**Interaction HLA*PFAS**
LPC(18:1)	0.003	0.012	0.067
LPC(18:2)	0.009	0.023	0.11
LPC(20:3)	0.002	0.034	**0.025**
LPC(20:4)	0.009	0.050	**0.041**
LPC(22:5)	0.31	0.0177	0.61
LPC(22:6)	0.0008	0.029	**0.025**
PC(40:8)	0.002	0.15	0.12
SM(d36:0)	0.002	0.035	0.084
SM(d36:0)	0.006	0.13	**0.012**
SM(d38:1)	0.0005	0.053	0.080
PC(O-38:4)	0.09	0.010	0.80

Supplementary Table 10. Top-ranking lipids affected by PFUnDA exposure in NOD mice.

Compound	p-value	FDR	Tukey's HSD	Fold 300 vs. 0	Fold 30 vs. 0	Fold 3 vs. 0
Cer(d18:1/24:0)	1.21E-02	7.75E-02	0 - 300; 3 - 300; 30 - 300	0.74	0.91	0.89
PC(18:0/18:0)	2.96E-03	4.32E-02	0 - 300; 3 - 300; 30 - 300	0.87	1.03	1.14
PC(32:2)	1.52E-04	1.32E-02	0 - 300; 3 - 300; 30 - 300	0.55	0.73	0.81
PC(33:2)	7.88E-05	1.32E-02	0 - 30; 0 - 300; 3 - 300; 30 - 300	0.61	0.81	0.96
PC(34:2)	1.97E-03	4.03E-02	0 - 300; 3 - 300; 30 - 300	0.86	0.93	0.99
PC(34:3)	1.11E-02	7.65E-02	0 - 300; 3 - 300; 30 - 300	0.68	0.82	0.85
PC(35:0)	3.27E-03	4.32E-02	0 - 30; 0 - 300; 3 - 30; 3 - 300	0.77	0.76	0.86
PC(35:2)	1.76E-03	4.03E-02	0 - 30; 0 - 300; 3 - 300; 30 - 300	0.73	0.87	0.89
PC(35:3)	1.58E-02	8.83E-02	0 - 30; 0 - 300; 3 - 300	0.68	0.90	0.93
PC(35:4)	1.99E-03	4.03E-02	0 - 30; 0 - 300; 3 - 30; 3 - 300	0.68	0.62	0.91
PC(36:2)	2.10E-03	4.03E-02	0 - 300; 3 - 300; 30 - 300	0.85	0.97	1.02
PC(36:2)	3.49E-03	4.32E-02	0 - 300; 3 - 300; 30 - 300	0.87	0.99	1.01
PC(36:4)	3.16E-03	4.32E-02	0 - 30; 0 - 300; 3 - 30; 3 - 300; 30 - 300	0.63	0.77	0.98
PC(36:4)	1.15E-02	7.65E-02	0 - 300; 3 - 30; 3 - 300	0.77	0.88	1.03
PC(37:4)	6.35E-03	6.11E-02	0 - 30; 0 - 300; 3 - 30; 3 - 300	0.67	0.77	1.02
PC(38:4)	3.96E-03	4.56E-02	0 - 300; 3 - 30; 3 - 300	0.72	0.87	1.06
PC(O-32:1)	1.84E-03	4.03E-02	0 - 300; 3 - 30; 3 - 300	0.84	0.90	1.12
PC(O-34:2)	1.59E-03	4.03E-02	0 - 300; 3 - 300; 30 - 300	0.76	0.88	0.98
PC(O-34:3)	9.24E-04	4.03E-02	0 - 300; 3 - 300; 30 - 300	0.80	1.09	1.14
PC(O-38:5)	7.74E-03	6.67E-02	0 - 30; 0 - 300; 3 - 30; 3 - 300	0.86	0.92	1.21
PC(O-38:5)	1.30E-02	7.77E-02	3 - 0; 3 - 30; 3 - 300	1.04	1.11	1.26
SM(d16:1/18:1) or SM(d18:2/16:0)	8.10E-03	6.67E-02	0 - 300; 3 - 30; 3 - 300; 30 - 300	0.89	0.96	1.06
SM(d18:0/16:0)	6.36E-03	6.11E-02	0 - 300; 3 - 300; 30 - 300	0.86	0.98	1.01
SM(d32:1)	8.91E-03	6.81E-02	0 - 300; 3 - 300; 30 - 300	0.85	1.02	1.04
SM(d33:1)	7.73E-03	6.67E-02	0 - 300; 3 - 300; 30 - 300	0.86	0.95	0.98
SM(d36:1)	1.30E-02	7.77E-02	3 - 0; 3 - 30; 3 - 300; 30 - 300	0.86	1.07	1.33
TG(52:6)	1.65E-02	8.93E-02	0 - 300; 3 - 300; 30 - 300	0.62	0.92	1.04
TG(52:7)	2.83E-03	4.32E-02	0 - 300; 3 - 300; 30 - 300	0.48	0.84	1.12
TG(53:6)	9.45E-03	6.81E-02	0 - 300; 3 - 300; 30 - 300	0.46	0.88	1.01
TG(54:5)	9.24E-03	6.81E-02	0 - 300; 3 - 300; 30 - 300	0.65	0.98	1.06
TG(54:7)	1.57E-02	8.83E-02	0 - 300; 3 - 300; 30 - 300	0.29	0.75	0.70
TG(60:7)	4.84E-03	5.24E-02	0 - 300; 3 - 300; 30 - 300	0.22	1.47	1.78

Supplementary Table 11. Top-ranking lipids and polar metabolites affected by exposure to POP mixture in NOD mice (low and high exposure levels).

Compound	p-value	FDR	Tukey's HSD	Fold high/ctrl	Fold low/ctrl
3-Hydroxybutyric acid	1.83E-10	5.68E-09	HIGH - CTRL; HIGH - LOW	3.88	1.18
Arachidonic acid	6.16E-09	9.55E-08	HIGH - CTRL; HIGH - LOW	0.54	0.93
Asparagine	5.24E-02	9.56E-02	HIGH - CTRL; HIGH - LOW	0.74	1.09
Aspartic acid	1.07E-04	5.53E-04	HIGH - CTRL; HIGH - LOW	0.75	0.94
CE(20:3)	3.71E-05	1.49E-04	HIGH - CTRL; HIGH - LOW	2.59	1.04
Cholesterol	6.99E-06	5.42E-05	HIGH - CTRL; HIGH - LOW; LOW - CTRL	0.49	0.76
DG(18:1/18:1)	1.67E-02	2.90E-02	HIGH - CTRL; HIGH - LOW	1.56	0.98
Fumaric acid	2.26E-02	5.28E-02	HIGH - CTRL; HIGH - LOW	1.56	0.98
Glutamic acid	3.52E-07	3.64E-06	HIGH - CTRL; HIGH - LOW	1.73	1.07
Glutamine	8.14E-03	2.29E-02	HIGH - CTRL; HIGH - LOW	0.52	1.13
Glycerol-3-phosphate	1.81E-04	8.01E-04	HIGH - CTRL; HIGH - LOW	0.57	0.75
Glycine	2.38E-02	5.28E-02	HIGH - CTRL; HIGH - LOW	0.80	0.99
Lactic acid	4.26E-03	1.47E-02	HIGH - CTRL; HIGH - LOW	1.16	0.90
Linoleic acid	3.88E-02	7.51E-02	HIGH - CTRL	0.62	0.85
LPC(16:0e)	6.41E-08	1.18E-06	CTRL - HIGH; LOW - HIGH	0.58	0.92
LPC(16:0p)	3.98E-08	1.18E-06	CTRL - HIGH; LOW - HIGH	0.37	0.77
LPC(16:1)	1.54E-03	3.53E-03	HIGH - CTRL; HIGH - LOW	1.31	0.83
LPC(18:0)	3.05E-03	6.38E-03	CTRL - HIGH; LOW - HIGH	0.88	1.18
LPC(18:1)	1.40E-03	3.31E-03	HIGH - CTRL; HIGH - LOW	1.26	0.89
LPC(20:3)	1.97E-06	1.25E-05	HIGH - CTRL; HIGH - LOW	3.14	1.07
LPC(20:4)	9.01E-08	1.31E-06	CTRL - HIGH; LOW - HIGH	0.53	1.06
LPC(22:5)	1.23E-11	2.27E-09	CTRL - HIGH; LOW - HIGH	0.29	0.98
LPC(22:6)	6.18E-08	1.18E-06	CTRL - HIGH; LOW - HIGH	0.54	1.05
LysoPE(18:1)	8.20E-03	1.52E-02	HIGH - CTRL; HIGH - LOW	1.15	0.87
Oleic acid	3.77E-02	7.51E-02	HIGH - LOW	0.88	1.18
Palmitic acid	6.64E-03	2.06E-02	HIGH - CTRL; HIGH - LOW	0.86	0.93
PC(16:0/16:0)	2.37E-04	6.93E-04	CTRL - HIGH; LOW - HIGH	0.70	0.89
PC(18:0/18:0)	1.15E-05	5.27E-05	CTRL - HIGH; LOW - HIGH	0.59	1.28
PC(18:0p/18:1)9Z	5.72E-06	3.19E-05	CTRL - HIGH; LOW - HIGH	0.44	1.00
PC(18:0p/22:6)	5.00E-07	3.84E-06	CTRL - HIGH; LOW - HIGH	0.31	1.15
PC(30:0)	5.87E-03	1.11E-02	CTRL - HIGH; LOW - HIGH	0.69	0.85
PC(31:0)	5.80E-04	1.55E-03	CTRL - HIGH; LOW - HIGH	0.47	0.97
PC(32:1)	3.71E-03	7.59E-03	CTRL - LOW; HIGH - LOW	1.13	0.77
PC(32:2)	1.15E-02	2.04E-02	CTRL - HIGH; CTRL - LOW	0.59	0.58
PC(33:1)	1.11E-02	1.98E-02	CTRL - HIGH; CTRL - LOW	0.67	0.70
PC(34:2)	4.00E-03	8.09E-03	CTRL - HIGH; CTRL - LOW	0.82	0.87
PC(34:1)	7.84E-05	2.83E-04	CTRL - LOW; HIGH - LOW	1.14	0.70

PC(34:3)	8.00E-04	2.07E-03	CTRL - LOW; HIGH - LOW	1.10	0.74
PC(35:2)	8.87E-08	1.31E-06	CTRL - HIGH; LOW - HIGH	0.50	0.97
PC(35:1)	2.18E-04	6.57E-04	CTRL - HIGH; LOW - HIGH	0.67	0.82
PC(35:3)	6.46E-04	1.70E-03	CTRL - HIGH; CTRL - LOW	0.84	0.74
PC(35:3)	1.09E-03	2.72E-03	CTRL - HIGH; LOW - HIGH	0.34	0.82
PC(36:1)	8.52E-05	3.02E-04	CTRL - HIGH; LOW - HIGH	0.74	1.00
PC(36:2)	9.36E-07	6.38E-06	CTRL - HIGH; LOW - HIGH	0.44	0.80
PC(36:2)	6.98E-05	2.57E-04	CTRL - HIGH; LOW - HIGH	0.75	0.99
PC(36:4)	3.81E-05	1.49E-04	HIGH - CTRL; CTRL - LOW; HIGH - LOW	0.61	0.92
PC(36:4)	6.19E-05	2.32E-04	CTRL - HIGH; CTRL - LOW; LOW - HIGH	1.19	0.74
PC(36:3)	8.79E-04	2.22E-03	HIGH - CTRL; HIGH - LOW	1.17	0.91
PC(37:4)	7.65E-10	4.88E-08	CTRL - HIGH; LOW - HIGH	0.29	1.05
PC(37:1)	1.19E-04	3.97E-04	CTRL - HIGH; LOW - HIGH	0.56	0.98
PC(37:2)	1.89E-05	8.08E-05	CTRL - HIGH; LOW - HIGH	0.67	1.01
PC(37:3)	4.54E-03	8.80E-03	CTRL - HIGH; LOW - HIGH	1.06	0.64
PC(38:2)	1.62E-07	1.76E-06	HIGH - CTRL; HIGH - LOW	2.53	1.11
PC(38:3)	3.37E-07	2.95E-06	HIGH - CTRL; HIGH - LOW	0.51	1.03
PC(38:4)	1.16E-06	7.63E-06	CTRL - HIGH; LOW - HIGH	0.43	0.96
PC(38:4)	6.17E-06	3.30E-05	CTRL - HIGH; LOW - HIGH	0.44	0.95
PC(38:5)	1.38E-07	1.59E-06	CTRL - HIGH; LOW - HIGH	0.58	0.98
PC(38:5)	8.12E-03	1.52E-02	CTRL - HIGH; LOW - HIGH	0.37	0.94
PC(38:6)	3.68E-07	3.08E-06	CTRL - HIGH; LOW - HIGH	0.50	0.98
PC(39:6)	6.09E-07	4.49E-06	CTRL - HIGH; LOW - HIGH	0.31	1.10
PC(40:4)	2.14E-02	3.64E-02	CTRL - HIGH; LOW - HIGH	0.77	1.10
PC(40:5)	6.16E-08	1.18E-06	CTRL - HIGH; LOW - HIGH	0.32	0.97
PC(40:6)	2.43E-07	2.36E-06	CTRL - HIGH; LOW - HIGH	0.32	0.97
PC(40:5)	1.14E-03	2.76E-03	CTRL - HIGH; LOW - HIGH	0.70	1.11
PC(40:6)	8.41E-04	2.15E-03	CTRL - HIGH; LOW - HIGH	0.58	1.03
PC(40:7)	4.29E-03	8.40E-03	CTRL - HIGH; LOW - HIGH	0.49	0.96
PC(40:8)	3.23E-05	1.32E-04	CTRL - HIGH; LOW - HIGH	0.45	1.01
PC(O-32:0)	4.69E-07	3.75E-06	CTRL - HIGH; LOW - HIGH	0.68	0.98
PC(O-32:1)	1.07E-05	5.04E-05	CTRL - HIGH; LOW - HIGH	0.50	0.86
PC(O-34:2)	3.06E-06	1.81E-05	CTRL - HIGH; LOW - HIGH	0.54	0.92
PC(O-34:3)	1.48E-03	3.45E-03	CTRL - HIGH; LOW - HIGH	0.44	0.64
PC(O-36:4)	6.45E-06	3.30E-05	CTRL - HIGH; LOW - HIGH	0.43	0.86
PC(O-36:5)	6.44E-06	3.30E-05	CTRL - HIGH; LOW - HIGH	0.34	0.74
PC(O-34:3)	1.55E-03	3.53E-03	CTRL - HIGH; CTRL - LOW	0.44	0.64
PC(O-38:4)	1.28E-07	1.57E-06	CTRL - HIGH; LOW - HIGH	0.35	0.89
PC(O-38:5)	2.41E-07	2.36E-06	CTRL - HIGH; LOW - HIGH	0.60	0.92
PC(O-38:5)	2.26E-04	6.71E-04	CTRL - HIGH; LOW - HIGH	0.49	1.11
PC(O-38:6)	2.42E-04	6.95E-04	CTRL - HIGH; LOW - HIGH	0.44	1.01

PC(O-38:6)	2.54E-02	4.25E-02	CTRL - HIGH; LOW - HIGH	0.48	1.12
PC(O-40:6)	1.11E-04	3.79E-04	CTRL - HIGH; LOW - HIGH	0.17	0.93
PC(P-18:0/22:6)	2.07E-03	4.58E-03	CTRL - HIGH; LOW - HIGH	0.52	0.92
PE(O-38:5) or PEp-38:4)	5.45E-03	1.05E-02	CTRL - HIGH; LOW - HIGH	0.80	0.91
PE(P-18:0/22:6)	1.80E-04	5.62E-04	CTRL - HIGH; LOW - HIGH	0.55	1.09
Serine	2.20E-02	5.28E-02	CTRL - HIGH	0.75	0.93
SM(d16:1/18:1) or SM(d18:2/16:0)	7.96E-10	4.88E-08	CTRL - HIGH; LOW - HIGH	0.61	1.13
SM(d18:0/16:0)	1.75E-05	7.68E-05	CTRL - HIGH; LOW - HIGH	0.46	1.10
SM(d18:1/24:0)	6.37E-08	1.18E-06	CTRL - HIGH; LOW - HIGH	0.61	1.00
SM(d32:1)	2.68E-06	1.64E-05	CTRL - HIGH; LOW - HIGH	0.48	1.00
SM(d33:1)	5.07E-08	1.18E-06	CTRL - HIGH; LOW - HIGH	0.61	1.08
SM(d34:1)	1.22E-07	1.57E-06	CTRL - HIGH; LOW - HIGH	0.48	1.12
SM(d36:1)	3.32E-06	1.91E-05	CTRL - HIGH; LOW - HIGH	0.45	1.06
SM(d36:2)	2.69E-07	2.47E-06	CTRL - HIGH; LOW - HIGH	0.51	0.94
SM(d38:2)	9.42E-06	4.68E-05	CTRL - HIGH; LOW - HIGH	0.74	0.98
SM(d40:1)	1.59E-03	3.57E-03	LOW - CTRL; LOW - HIGH	0.45	1.12
SM(d41:1)	3.82E-08	1.18E-06	CTRL - HIGH; LOW - HIGH	0.50	1.05
SM(d42:2)	7.61E-07	5.39E-06	CTRL - HIGH; LOW - HIGH	0.40	1.03
Stearic acid	4.51E-05	2.79E-04	HIGH - CTRL; HIGH - LOW	0.76	1.12
TG(14:0/16:0/18:1)	1.31E-04	4.30E-04	HIGH - CTRL; HIGH - LOW	2.47	0.73
TG(14:0/18:1/18:1)	9.66E-06	4.68E-05	HIGH - CTRL; CTRL - LOW; HIGH - LOW	1.91	0.77
TG(14:0/18:2/18:2)	2.03E-04	6.23E-04	HIGH - CTRL; HIGH - LOW	2.09	1.14
TG(16:0/16:0/16:0)	1.17E-03	2.79E-03	HIGH - CTRL; CTRL - LOW; HIGH - LOW	1.28	0.71
TG(16:0/18:0/18:1)	9.94E-03	1.81E-02	HIGH - LOW	1.17	0.85
TG(18:1/12:0/18:1) or TG(18:2/16:0/14:0)	1.23E-05	5.50E-05	HIGH - CTRL; CTRL - LOW; HIGH - LOW	2.38	0.69
TG(18:1/18:1/16:0)	3.97E-04	1.11E-03	HIGH - CTRL; HIGH - LOW	1.66	0.80
TG(18:1/18:1/18:1)	2.45E-03	5.31E-03	HIGH - CTRL; HIGH - LOW	1.53	1.04
TG(18:1/18:1/22:6)	2.67E-03	5.71E-03	CTRL - HIGH; LOW - HIGH	0.43	1.23
TG(18:2/18:1/16:0)	1.69E-02	2.90E-02	HIGH - LOW	1.14	0.97
TG(18:2/22:5/16:0)	1.41E-02	2.47E-02	CTRL - HIGH; LOW - HIGH	0.57	1.34
TG(480	2.17E-03	4.76E-03	HIGH - CTRL; HIGH - LOW	1.35	0.81
TG(48:1)	1.53E-04	4.94E-04	HIGH - CTRL; HIGH - LOW	2.19	0.84
TG(48:1)	9.24E-05	3.21E-04	HIGH - CTRL; HIGH - LOW	2.62	0.94
TG(49:2)	2.31E-02	3.90E-02	HIGH - LOW	1.29	0.86
TG(50:5)	9.10E-03	1.67E-02	HIGH - CTRL; HIGH - LOW	2.35	0.72
TG(50:1)	1.75E-04	5.54E-04	HIGH - CTRL; CTRL - LOW; HIGH - LOW	1.74	0.76
TG(50:2)	2.17E-05	9.08E-05	HIGH - CTRL; CTRL - LOW; HIGH - LOW	1.54	0.76

TG(50:3)	2.81E-04	7.96E-04	HIGH - CTRL; HIGH - LOW	2.15	1.02
TG(50:3)	5.04E-04	1.39E-03	HIGH - CTRL; HIGH - LOW	2.00	0.95
TG(50:5)	1.13E-03	2.76E-03	HIGH - CTRL; HIGH - LOW	2.35	0.72
TG(51:2)	1.04E-02	1.88E-02	CTRL - LOW; HIGH - LOW	1.45	0.80
TG(52:6)	2.84E-02	4.72E-02	HIGH - CTRL	2.81	2.35
TG(52:2)	5.65E-04	1.53E-03	HIGH - CTRL; HIGH - LOW	1.45	0.80
TG(54:2)	3.30E-03	6.81E-03	HIGH - LOW	1.24	0.90
TG(54:2)	4.07E-03	8.13E-03	CTRL - LOW; HIGH - LOW	1.31	0.95
TG(54:3)	4.14E-03	8.19E-03	HIGH - CTRL; HIGH - LOW	1.42	1.03
TG(58:6)	2.95E-03	6.24E-03	CTRL - HIGH; LOW - HIGH	0.61	0.90
TG(58:9)	4.53E-05	1.74E-04	CTRL - HIGH; LOW - HIGH	0.28	1.45
Threonine	1.90E-03	7.37E-03	CTRL - HIGH; LOW - HIGH	0.61	0.97